Summer 2011

Dissolution and aggregation of zinc oxide nanoparticles at circumneutral pH; a study of size effects in the presence and absence of citric acid

R-A-Thilini Perera Rupasinghe
University of Iowa

DISSOLUTION AND AGGREGATION OF ZINC OXIDE NANOPARTICLES AT CIRCUMNEUTRAL pH; A STUDY OF SIZE EFFECTS IN THE PRESENCE AND ABSENCE OF CITRIC ACID

by

R-A-Thilini Perera Rupasinghe

A thesis submitted in partial fulfillment
of the requirements for the Master of Science
degree in Chemistry
in the Graduate College of
The University of Iowa

July 2011

Thesis Supervisor: Professor Vicki H. Grassian

Graduate College
The University of Iowa
Iowa City, Iowa

CERTIFICATE OF APPROVAL

_____

MASTER'S THESIS

_____

This is to certify that the Master's thesis of

R-A-Thilini Perera Rupasinghe

has been approved by the Examining Committee
for the thesis requirement for the Master of
Science degree in Chemistry
at the July 2011 graduation.

Thesis Committee: _____
Vicki H. Grassian, Thesis Supervisor

_____
Sarah C. Larsen

_____
Edward Gillan

To my ever loving “Amma” (mother),
not only for being my mother, but also for teaching me the “Abc ” in chemistry.
As I believe, you are the giant shade behind my success.

ACKNOWLEDGMENTS

I would like to thank my advisor, Professor Vicki H. Grassian, for supporting me during last one and half years in several ways. Upon everything thing I am grateful to her for helping me to wake up the “strong woman” inside me. Your “words and decisions” made me became stronger in my academic life.

Many thanks also to my committee members, Professors Sarah Larsen, Ed Gillan, for all of your support. A special thank you goes to all the members of Grassian research group specially Dr. Larissa Stebanovna, Dr. Shaowei-bian, Chia-ming Wu, Gayan Rubasinghege and Imali Mudunkotuwa for their valuable support.

I would also like to mention all my teachers since my high school time for showing me the correct path in my life. Next, I would like to thank all my friends for their valuable support. All of you were there for me in my “ups and downs” and your words encouraged me a lot to achieve my goal.

A special thank goes to my family. Their support was so precious. I should specially mention my mother; you were my first ever chemistry teacher. Thank you very much for showing me the “beauty” of chemistry when I was a small kid. Finally, thanks to my loving Lahiru for his kind, valuable support. You were with me days and nights when I was working in the lab. Honestly, I don’t have words to express my thanks to you for everything you have done for me.

ABSTRACT

Understanding the size dependent dissolution of engineered nanoparticles is one important aspect in addressing the potential environmental and health impacts of these materials as well as their long-term stability. In this study, experimental measurements of size dependent dissolution of well-characterized zinc oxide (ZnO) nanoparticles with particle diameters in the range of 4 to 130 nm have been measured and compared at circumneutral pH (pH 7.5).

Enhanced dissolution was found for the smaller particles with the largest enhancement observed in Zn^{2+}(aq) concentrations for 4 nm diameter ZnO nanoparticles compared to larger-sized particles. Interestingly, size dependent dissolution was observed even though the nanoparticles aggregated with hydrodynamic diameters on the order of 1-3 μm in diameter. Although these results are found to be in qualitative agreement with theoretical predictions used to predict the dissolution of solids, a linearized form of the Kelvin equation to calculate a bulk dissolution value for ZnO and a surface free energy yielded quantities inconsistent with known literature values. It is therefore concluded that deviations from solubility behavior from classical thermodynamics are due to a lack of the detailed knowledge of the surface free energy as well as its dependence on the details of the surface structure, surface properties, including the presence of different surface crystal facets and adsorbed ligands, as well of aggregation state.

The presence of citric acid significantly enhances the extent of ZnO dissolution for all sizes such that no significant differences were observed for total Zn^{2+}(aq) concentrations for nanoparticles between 4 to 130 nm. This can be attributed to ligand enhanced dissolution of ZnO nanoparticles where there is no dependence on size.

Adsorption of citrates onto ZnO nanoparticles was observed using ATR-FTIR spectroscopy. A reversal of surface charge of ZnO nanoparticles was observed upon adsorption of citrates. Adsorption of negatively charged Cit^{3-} onto ZnO nanoparticles make the surfaces negatively charged and this result in a repulsion between nanoparticles eventually leading to a lesser extent of aggregation. Formation of a stable suspension was also observed in the presence of citric acid. These trends observed in aggregation pattern are of great environmental and biological importance as citric acid is abandon in the environment as well as in human body.

TABLE OF CONTENTS

LIST OF TABLES

Table

LIST OF FIGURES

Figure

CHAPTER-1

INTRODUCTION

Nanotechnology has been subject to numerous discussions and developments during last few decades, starting from Richard Feynman's speech in 1959, followed by the introduction of the word "Nanotechnology" in 1974 by Norio Taniguchi. Although materials in the nanoscale size regime have been present for millions of years,[1] these nanomaterials have attracted a greater deal of attention recently owing to the fact that they show distinct properties arising due to size, morphology and they can now be synthesized with great control.[2] As a result, a large number of materials having nanoscale dimensions are being used because of their unique electronic, thermal, optical and photoactive properties in the fields of information technology, catalysis and medicine.[3-7]

One key aspect of nanoscience is the ability to tune the properties of materials via the control of size and shape.[8-12] For example, it was clearly demonstrated in a number of studies that electronic properties exhibit size-dependent behavior.[8,10] Additionally, magnetic properties of transition metals have shown significant variations with size when materials are in the nanoscale size regime.[10] Theoretical calculations have shown that the surface charge density of nanomaterials are highly size dependent whereby a considerable increase in surface charge density is predicted for particles smaller than 10 nm.[9] Chemical reactivity and catalytic activity of nanomaterials also depend on size where smaller nanomaterials are often more active and show enhanced selectivity compared to their larger counterparts.[10,13]

1.1 Types of engineered nanoparticles

Engineered nanoparticles (ENPs) are generally classified based either on their composition, size or morphology. However, with respect to their composition, they can be broadly categorized as fullerenes, carbon nanotubes, metal ENPs, metal oxide ENPs, organic polymer ENPs and quantum dots.[14]

Fullerenes are basically made up of pure carbon and examples include bucky balls and endofullerenes. Carbon nanotubes (CNTs) are fibrous fullerenes consisting of rolled graphine sheets and have attracted a great deal of attention since their discovery in 1992 by Japanese scientist Sumio Lajima. CNTs are widely used in applications such as electronics and optics due to their unique electrical properties, high thermal conductivity, mechanical strength and hydrophobicity. Quantum dots are fluorescent semiconductor nano dots mainly having CdSe, CdS and PbSe cores. These can emit light as their size is smaller than Bohr excitation radius and are widely used in medical applications.[14]

Nanoparticulate metal oxides are among the most widely used ENPs having applications in the fields such as medicine, cosmetics and textile. Few examples of such metal oxide nanoparticles are ZnO, TiO_2 and Al_2O_3. ZnO ENPs are used in sunscreens, electronics and antimicrobial agents while TiO_2 is mainly used in memory chips and catalysis.[15] Organic polymer ENPs are generally developed as micelles and liposomes for pharmaceutical products especially in drug delivery.

1.2 Reactivity of nanoparticles

Nanoparticles differ significantly from the bulk as they can show different reactivities and properties. As a result of decreasing size, number of surface atoms increases eventually leading to a higher surface to volume atomic ratio leading to a higher reactivity.[16] Table 1.1 shows the variation of surface atoms with decreasing size. Atoms on a surface possess only few neighboring atoms and are coordinatively unsaturated. Hence they are extremely reactive and larger number of surface atoms results in an enhanced reactivity.

Table 1.1: Number of surface atoms and percentage of atoms on the surface of GaAs nanoparticles with decreasing size[17]

Size (nm)	Total number of atoms	Number of surface atoms	Percent of atoms on surface
1.13	94	48	51.1 %
2.26	620	192	31.0 %
3.39	1962	432	22.0 %
8.48	2.84×10^4	2700	9.5 %
14.1	1.29×10^5	7500	5.8 %
28.3	1.02×10^6	3.0×10^4	2.9 %
56.5	8.06×10^6	1.2×10^5	1.5 %

In a thermodynamic point of view, the total free energy of a particle can be written as the sum of the free energy of the bulk and the surface of nanoparticle. (Eq 1)

$$G_{nanoparticle} = G_{surface} + G_{bulk} \quad (1)$$

For nanoparticles, $G_{surface}$ is nearly 25 % of the G_{bulk} and hence it has a significant contribution for the total free energy of the nanoparticle. This is due to the increase in surface area and percentage of surface atoms with decreasing particle size.[16] Hence, the total free energy of nanoparticles increases with decreasing particle size resulting in higher reactivity. Properties associated with bulk materials on the other hand have properties such as density, resistivity and dielectric constant with little contribution from the surface atoms.[17] Therefore bulk materials do not exhibit such a dramatic dependence on size.

1.3 Fate of engineered nanoparticles

Today, engineered nanoparticles are widely used in number of consumer products, as a result of above distinct properties. According to nanomaterials market research report released in 2010, annual global nanomaterial demand is increasing by a factor of 21 % and by 2025, nanomaterials are expected to reach over $ 34 billions in sales.[18] With this huge consumption, there is a high possibility of their release into the environment during production, transport and use. This can result in adverse health and environmental problems. Once released, these novel particles can undergo different modifications as shown in Figure 1.1. Nanoparticles which are released in the free form

can undergo aggregation forming larger particles eventually end up in aquatic system upon dissolution. Nanoparticles which are not released as free nanoparticles can undergo different surface modifications in the presence of light and microorganisms and form free nanoparticles. These newly formed free nanoparticles can also follow the same routine and end up in the aquatic system as dissolved ions, colloids or humic substances.

In addition, these novel particles can enter soil system and atmosphere and their presence in the environment leads to a higher degree of human exposure.[1] For example, it has been revealed from number of studies that air contains 10,000 – 15,000 particles per cubic centimeter which are in the nanoscale size regime.[14] Soil also contains a significant amount of nanoparticles, where high surface area and abundance of charged and hydrophobic adsorption sites make soil a good reservoir for engineered nanoparticles.

In the environment ENPs can also be transformed into different species through abiotic transformations such as redox transformations, photolysis and biotransformations such as aerobic oxidations and anaerobic reductions.[19] Different surface modifications such as surface functionalization can take place on ENPs once they are present in the environment. Few example of such surface functionalization are sorption of dissolve or natural organic matter (DOM/ NOM) and hydroxylation of fullerenes to fullerols.

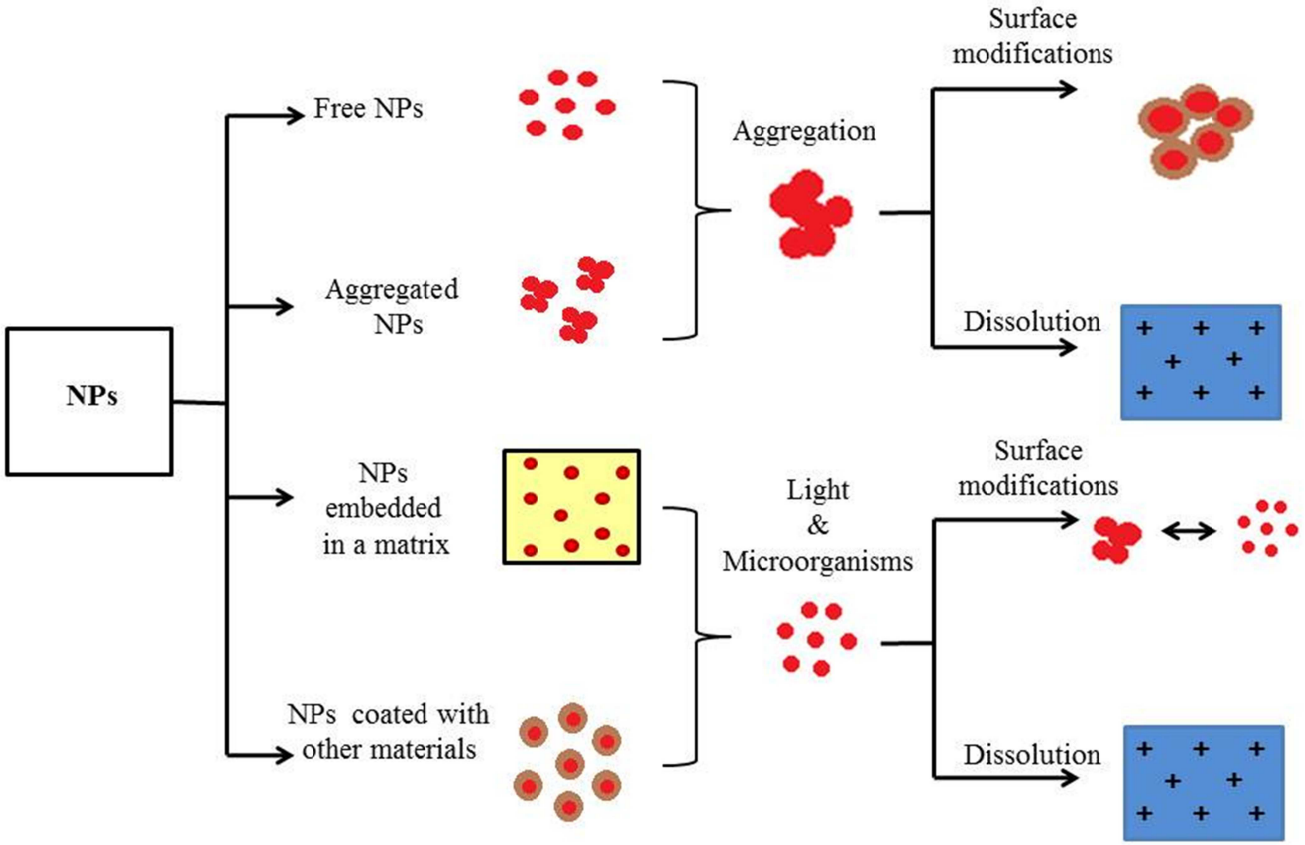

Figure 1.1: Fate of engineered nanoparticles once they are released to the environment

Some of the ENPs can get oxidized once they are present in the atmosphere and oxidation of diesel soot is a good example. Loss of surface coating of ENPs upon biodegradation is also a common situation that can take place and this can result in free ENPs with a high surface energy. These free ENPs will undergo aggregation reducing their high surface energy. Larger aggregates tend to settle down easily due to gravitational forces and this will result in a higher bio availability of ENPs in soil and sediments. Their propensity to form aggregates will limit the mobility of ENPs.

Released ENPs can also be transported into ground waters and result in adverse effects. However, geochemical conditions such as pH, ionic strength and ionic composition can affect the extent of these processes in the environment controlling the fate and transportation of ENPs.

Dissolution is one of the major pathways from which people are exposed to nanoparticles. Nanoparticles being a novel group chemicals show different properties compared to the bulk, for example they show different degree of toxicity relative to the bulk. It has been found from several studies that metal oxide nanoparticles such as ZnO, TiO_2 and Fe_2O_3 can show toxicity such as inflammatory response and cell membrane leakage once they enter the human body.[5]

1.4 Size dependent dissolution of nanoparticles

Size dependent dissolution of nanomaterials is an area of great interest due to the importance of dissolution in industries such as pharmaceuticals, cosmetics and agrochemical.[20,21] Significant increases in solubility with decreasing particle size have been reported.[4,13,20,22] Pharmaceutical drugs composed of nanoscale particles are

considered an important formulation route for oral administration of drugs having poor dissolution properties.[20] Furthermore, it is now becoming clear that the dissolution of engineered nanomaterials is extremely important in terms of stability of these metals as well as the environmental and health impacts that these particles may have if released into the environment.[23] Dissolution of nanoparticles in aqueous systems, especially for metal-based nanomaterials, is a concern because these metals can give rise to toxic effects.[24] Since the properties of nanoscale materials differ markedly from the bulk, variations in toxicity effects may be expected for nanomaterials relative to micron-sized particles of these materials.[25]

Dissolution of materials has long been studied where an enhanced dissolution of finely divided solids compared to large crystals were observed.[26,27] Increased surface area is one important reason for increased kinetic rates of dissolution. For very small particles several theoretical models and approaches have been put forth to describe the size dependent dissolution of materials beyond surface area effects.[21,28] However, large discrepancies exist among these theoretical studies and experimental measurements in addition to only a limited number of investigations being available on well characterized nanomaterials to describe this phenomenon.

1.5 Aggregation of nanoparticles

Nanoparticles tend to attract each other through chemical bonds or physical interaction forces at interfaces forming larger particles in order to reduce high surface energy and the phenomenon is named as aggregation.[16] This is an important topic in most of the industrial applications where aggregation can decrease the efficiency of

certain reactions which are important in industry. Thus reagents such as dispersants are added to nanoparticle suspensions to prevent aggregation.

Total interaction between two particles can be expressed in terms of van der Waals attractions and electrostatic repulsions as follows.

$$V_{total} = V_{attractive} + V_{repulsive} \quad (2)$$

This electrostatic interaction is successfully described by the DLVO (Derjaguin, Landdau, Verwey and Overbeek) theory.[16,29,30] According to the theory, when the distance between the surfaces of the two particles is larger than the combined thickness of the electrical double layers of the two particles, there would be no overlap of the diffusion double layers. When particles approach each other, two double layers can overlap and a repulsion force is developed as shown in Figure 1.2.

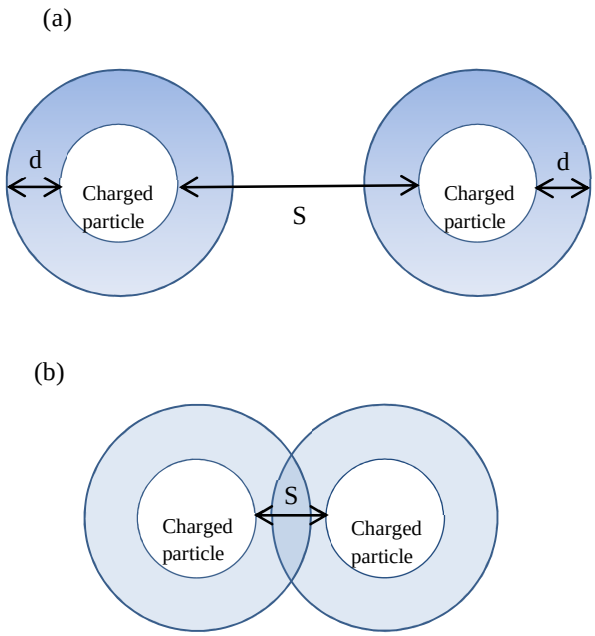

Figure 1.2: Schematic representation of nanoparticle-nanoparticle interactions. (a) Distance between particles is larger than the double layer thickness and no overlap. (b) With decreasing distance, particles reach each other forming aggregates.

Particles having sufficient energy to overcome the energy barrier which is created by repulsive forces will form aggregates. Nanoparticle aggregation plays a significant role in determining the fate and transport of ENPs where limited bio availability is resulted upon aggregation.

1.6 Zinc oxide nanoparticles

Zinc oxide (ZnO) is an inorganic compound which is widely used in a number of applications and occurs as a white powder known as mineral “Zincite”. This has mainly three crystal forms namely wurtzite, zincblend and rock salt. Out of these three phases, wurtzite is the most stable at room temperature. Properties such as high thermal conductivity, heat capacity and melting point have made ZnO a good candidate in ceramic industry.[31,32] As a result of high band gap, ZnO is widely used in electronics and Table 1.2 summarizes some of the important properties of ZnO.[13,33]

Table 1.2: Distinct properties of zinc oxide

Property	Value
Band gap	3.37 eV
Binding energy	60-80 meV
Melting point	1975 ˚C
Refractive index	2.0041

Nanoscale ZnO is of particular interest as it is widely used in a number of consumer products such as cosmetics, dye sensitized cells, plastic additives and electronics due to its distinct thermal, electronic and optical properties.[12,34-38] Currently ZnO nanostructures are synthesized in a variety of morphologies such as nanorods, nanowires, nanoparticles and tetrapods via a wide range of processes such as wet chemical, template induced methods and hydro thermal processes.[39]

In cosmetics industry, ZnO nanoparticles are highly used in sunscreen creams and anti-microbial agents. Due to its band gap is in the UV range, ZnO acts as a good UV blocking agent. The anti-microbial activity of ZnO is achieved via formation of reactive oxygen species (ROS). Nanorod arrays of ZnO are used in various photoelectric systems such as nanolasers, schottky diodes, bio sensors and solar cells.[40] Thin films of nano ZnO play an important role in drug delivery and medicinal applications. In addition ZnO nanotubes are used in dye sensitized solar cells. Therefore ZnO can be named as one of the most extensively used class of nanomaterials.[41] Thus occupational, incidental and direct exposure via consumption can be given as the most likely routes of exposure to ZnO ENPs.

1.7 Toxicity of ZnO nanoparticles

Despite the general conviction of ZnO as a biologically safe material, recent research continues to highlight potential biological toxicities of nanoscale ZnO and a summary is presented in Table 1.3.

Table 1.3: A brief summary of toxicity studies of ZnO nanoparticles.

Study	Focus	Results
Brayner *et. al.*[2]	Biocidal effects and cellular internalization of nanoscale ZnO in *E.coli.*	Membrane disorganization resulting in increased permeability and accumulation of ZnO NPs in the bacterial membrane was observed.
Adams *et. al.*[42]	Toxicity of TiO_2, SiO_2 and ZnO towards *Bacillus subtilis* and *E.coli*.	ZnO is the most toxic out of three metal oxide ENPs.
Lin *et. al.*[43]	Comparison of the toxicity of ZnO and Zn^{2+} with *Lotium perenne*.	ZnO showed more toxicity than Zn^{2+}
Heinlann *et. al.*[44]	Determination of LC_{50} (mg/L) of ZnO ENPs for *Vibrio fischeri*, *Daphina magna*, *Thamnocephalus*.	LC_{50} values are 1.9, 3.2 and 0.18 mg/L respectively.
Xia *et. al.*[45]	Cellular response of macrophage and epithelial cell lines towards ZnO ENPs.	Upon dissolution of ZnO, Zn^{2+} is released inducing toxicity. Size reduction of agglomerates was observed.
Raghupathi *et.al.*[46]	Size dependent growth inhibition of microorganisms with ZnO suspensions.	Toxicity is due to ZnO not Zn^{2+} ions.

However, many controversies still exist on the origin of these toxicities generation of reactive oxygen species (ROS), creations of protein corona encapsulating the nanoparticles (depending on size, curvature, shape and surface features) leading to protein unfolding, fibrillation, thiol cross linking and loss of enzymatic activity. [45] The debate among the scientific community in determining the toxicity mechanisms of nanoscale ZnO still continues. Therefore fundamentally understanding size dependent dissolution of nanoscale ZnO becomes crucial with respect to environmental and toxicological perspective.

1.8 Significance of citric acid

Citric acid (Figure 1.3 a) is a naturally occurring tri carboxylic acid with pK_{a1} = 3.13, pK_{a2} = 4.76, pK_{a3} = 6.40. It is highly abundant in the environment and has both natural as well as anthropogenic sources. Citric acid is an important intermediate in biological processes such as oxidation of fats, carbohydrates and proteins. It is a natural preservative, anti-oxidant and a benign cleaning agent and involve in detoxification of metals, mineral dissolution and acquisition of nutrients from plants.[30,47]

In industry citric acid is used as a food additive in flavoring and as a preservation agent, water softening and in stainless steel passivation. It is also used in a wide range of effervescent formulae such as personal care products and ingestion of tablets.[47]

(a)

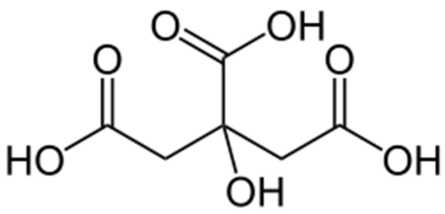

(b)

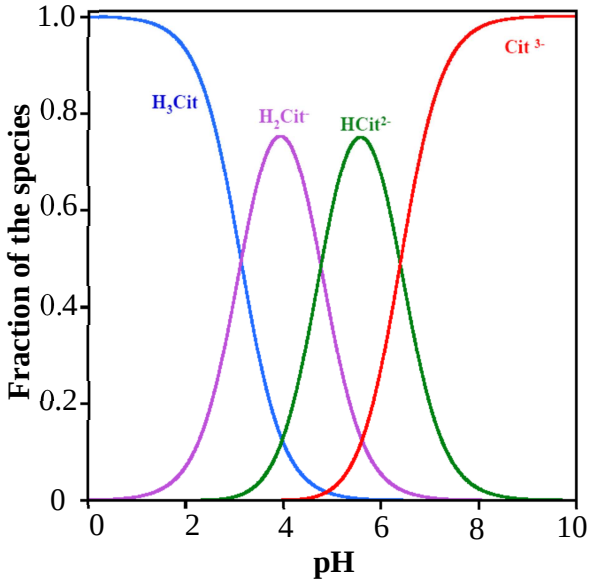

Figure 1.3: Citric acid

(a) Structure (b) Calculated speciation of citric acid as a function of pH.

Citric acid can form different species depending on solution pH as shown in figure 1.3(b). In nano industry, citric acid is often used in nanoparticle synthesis to control the size and morphology. [30,48-50] Citrate ion can undergo facile exchange with other surface functional groups and this makes citrate a good ligand in preparation of nanomaterials. Citric acid is also present in human plasma (0.1 M) and interacts with foreign species which are entering the body.[51]

Once ENPs are released to the environment there is a high possibility of their interaction with organic acids. The estimated total organic acid concentration in rhizosphere is 1 mM and this being a significant number, support the fact that ENPs can

easily interact with organic acids. Citric acid is a good example of such organic acids and therefore citric acid based studies are considered to be good analogs for studying the interactions between ENPs and complex organic acids such as humic acid.

Studying the adsorption of citric acid onto ENPs and effect of citrate towards the dissolution, aggregation and stability of ENPs can provide a better insight into the interactions between ENPs and complex organic systems. Presence of citric acid inside the body makes it even more important.

The main focus of this research is to better understand the fate and behavior of ZnO nanoparticles in the environment. Size dependent dissolution of well characterized ZnO nanoparticles in the range of 4-130 nm is studied to understand the dissolution process on the nanoscale. Although several studies have been reported in literature on dissolution of ZnO nanoparticles, only a limited number of studies have been conducted on well characterized nanoparticles. Thus, this current study becomes important in understanding size dependent behavior. Secondly, the effect of natural organic acids towards the behavior of ZnO nanoparticles in the aquatic system is also studied. Citric acid being a good example of natural organic acids is used to study the effect of organic acids towards the stability and behavior of ZnO nanoparticles in the aqueous system. Adsorption of various natural organic compounds onto the surface of nanoparticles can completely change their behavior and therefore, studying the adsorption of such compound onto the surfaces of nanoparticles is essential. Overall, this research is enormously important in studying the fate and behavior of nanoparticles in aquatic system and environment.

CHAPTER 2

EXPERIMENTAL SECTION

2.1 Materials

Several different types of ZnO nanomaterials were used in this study which included six laboratory synthesized samples and a commercially manufactured sample. The detailed synthesis of ZnO powdered materials can be found in Bian et al. for the 4 nm diameter ZnO and in Wu et al. for 7, 17, 24, 47 and 130 nm diameter ZnO samples.[13,52] The commercial ZnO nanoparticles of 15 nm diameter was purchased from Alfa Aesar.

For the dissolution studies, solutions at pH 7.5 were prepared with 4-(2-hydroxyehtyl)-piparazeneethanesulfonic acid (HEPES; Sigma Aldrich; ≥ 99%). To adjust the pH of the solution to 7.50 ± 0.01, sodium hydroxide (NaOH; Fisher Scientific; certified ACS plus) was used. Citric acid (Sigma Aldrich, 99.5% certified ACS plus) and other solutions were prepared using optima water (Fisher Scientific). Sodum chloride (NaCl; Fisher Scientific; certified ACS plus) was used to adjust the ionic strength.

2.2 Characterization of ZnO nanoparticles

Nanoparticles used in this study were characterized with different techniques such as transmission electron microscopy (TEM), powder X-ray diffraction (XRD), BET surface area analysis and ATR-FTIR spectroscopy as described in detail previously.[13,52] Briefly, powder X-ray diffraction (XRD) was used to determine the bulk crystalline

phase of ZnO nanoparticles. Diffraction patterns were collected using a Rigaku Miniflex II diffractometer with a Co source. Transmission electron microscopic images of the samples were collected using TEM, JEM JEOL-1220. The specific surface area of the particles was measured using seven-point N_2 BET adsorption isotherm measurements using a Quantachrome Nova 4200e surface area analyzer. Measurements are reported as the average of triplicate measurements. Attenuated total reflectance Fourier transform infrared (ATR-FTIR) spectroscopy measurements were obtained to investigate the surface functional groups present on ZnO nanoparticles. Measurements were obtained using AMTIR crystal element in a horizontal ATR cell (Pike Technology, Inc.). A thin film of ZnO was prepared by depositing a ZnO suspension (1.5 mg in 1.0 cm^3 of ethanol) onto the AMTIR crystal and dried overnight. ATR-FTIR spectra of the thin films of nanoparticles were recorded.

2.3 Quantitative dissolution measurements

Dissolution studies were conducted using Varian inductively coupled plasma optical emission spectrophotometer (ICP-OES) at room temperature (~25°C) at pH 7.5. This solution contained HEPES (4-(2-hydroxyethyl)-1-piperazineethanesulfonic acid) and experiments were conducted according to the following protocol.[29,30] Dissolution at pH 7.5 was studied using seven ZnO samples of sizes 4, 7, 15, 17, 24, 47 and 130 nm with a solid loading of 0.5 g/L. ZnO and pH 7.5 buffer prepared in optima water were mixed in a 20 ml vial and then covered with aluminum foil to inhibit any photo-induced dissolution. This vial was then placed on a Cole-Parmer circular rotator for 24 hours. After completion of mixing, suspension pH was measured. From each reactor three

aliquots (~ 1 ml each) were drawn out with a disposable syringe, passed through a 0.2 μm syringe-driven filter (Xpertek) into centrifugation vials, and centrifuged at 22000 rpm for 30 min to separate the solution from ZnO nanoparticles. Samples were analyzed using a Varian 720-ES inductively coupled plasma optical emission spectrophotometer (ICP-OES) to quantify dissolved zinc. These centrifuged samples were diluted to 5 ml with 1 M HCl prior to analysis and the calibration was conducted with 5.0, 10.0, 25.0, 50.0 and 100 ppm Zn^{2+} standards prepared in 1 M HCl. The average and standard deviation of triplicate measures are reported for all dissolution measurements. Similar ICP-OES analysis of ca. 4 nm TiO_2 nanoparticles has shown that filtration followed by centrifugation successfully remove all non-dissolved nanoparticles from the medium.[29,30]

Dissolution rates of ZnO NPs of different sizes were investigated in a kinetic study using 4, 7 and 15 nm ZnO samples. The above procedure was followed with aliquots of sample being drawn at time intervals of 2 minutes for the first 30 minutes followed by 15 minutes intervals for next 4 hours and then 1 hour intervals for 24 hours. These data showed that the dissolution of ZnO nanoparticles at this pH reach steady state in 24 hours.

Another set of experiments were conducted in the presence of citric acid to study the effect of complexing agents towards the dissolution of ZnO nanoparticles. Same procedure was followed and citric acid solutions were prepared in HEPES medium and the initial pH was adjusted to 7.5 using 4.2 M NaOH.

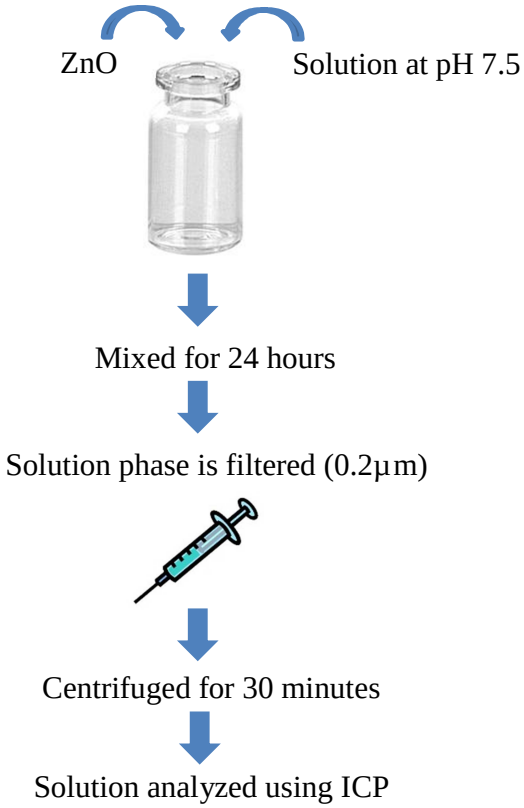

Figure 2.1: Schematic representation of the experimental procedure for the dissolution studies.

2.4 Adsorption studies – ATR-FTIR spectroscopy

Adsorption of citric acid onto ZnO nanoparticles was studied using attenuated total reflectance fourier transform infrared (ATR-FTIR) spectroscopy. Solution phase spectra for 100 mM citric acid at pH 7.5 were recorded using a Thermo-Nicolete FTIR spectrometer equipped with a MCT-A detector.

For surface adsorption studies, a thin, evenly coated ZnO film was deposited onto an AMTIR crystal element in a horizontal ATR cell (Pike Technologies, Inc.). Film was prepared by placing a suspension of ZnO (1.5 mg in 1 mL of Optima water) onto the crystal and drying overnight. The deposited film was slowly flushed with a stream of water to eliminate any loosely bound particles. Citric acid solution (5 mM) prepared at pH 7.5 was then introduced into horizontal cell and the spectra were collected in 5 minutes intervals for 2 hours in the spectral range 500 cm^{-1} to 4000 cm^{-1} at an instrument resolution of 4 cm^{-1}.

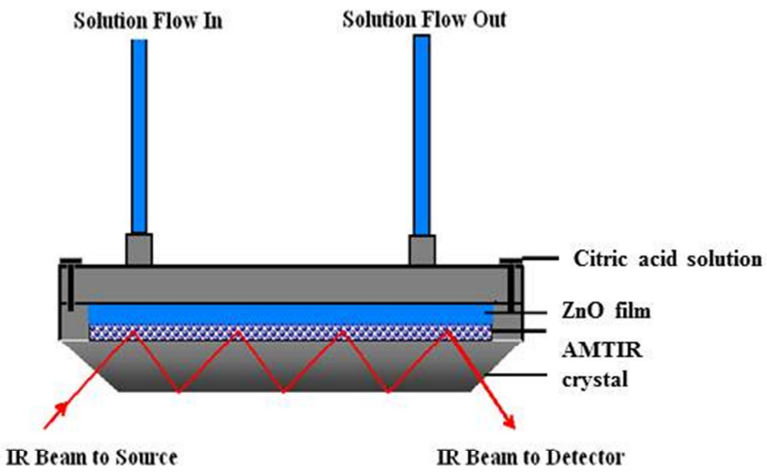

Figure 2.2: Recording of surface spectra using ATR-FTIR spectroscopy. IR beam undergoes multiple internal reflections as shown.

2.5 Surface charge measurements

Surface charge of the nanoparticles was measured using the zeta potential mode of the Malvern Zetasizer Nano ZS. Suspensions having a solid loading of 0.02 g/L were prepared in the presence (0.3 – 5.0 mM) as well as in the absence of citric acid and were allowed to equilibrate for 24 hours to reach the steady state. Surface charge measurements were obtained for samples of sizes 4,7 and 15 nm. In addition another set of experiments were conducted with to determine the point of zero charge of ZnO samples (4 and 15 nm) using a series of pHs.

2.6 Nanoparticle- nanoparticle interactions

Once present in a solution, ZnO nanoparticles can attract each other and form larger aggregates as described under section 1.5. This phenomenon is very important in understanding the fate and behavior of ENPs in the environment. Different environmental conditions such as presence of organic acids and ionic compounds can affect the aggregation process and such effects are studied under section 2.6.

2.6.1 Quantitative measurements

- **Dynamic light scattering technique**

Because of the propensity of nanoparticles to aggregate and the impact that aggregation may have on dissolution,[53] the aggregation behavior of ZnO particle suspensions were examined. Size distributions of the aggregates were obtained using a

dynamic light scattering (DLS) instrument (Delsa Nano C particle analyzer) equipped with a green laser at 532 nm. For DLS measurements suspensions were prepared at 0.5 g/L solid loading of ZnO at pH 7.5. Initially, the solution at pH 7.5 was passed through a 0.2 μm syringe driven filter to minimize the effect of unwanted dust particles. Samples were allowed to sit overnight to ensure the aggregates had reached its steady state and size distributions were measured for all the samples.

Effect of citric acid towards the aggregation and stability of ZnO nanoparticles was studied in the presence of citric acid (0.3 – 5.0 mM). Same procedure was followed and samples were analyzed using DLS.

2.6.2 Qualitative measurements - Sedimentation experiments

Sedimentation experiments were conducted with a UV-Vis spectrometer by monitoring the changes in the light scattering when passed through ZnO suspensions (0.5 g/L) as a function of time at a wave length of 378 nm.[34] Same solid loading was used as in DLS experiments and measurements were taken after 24 hours. ZnO suspensions were prepared in a 1 cm path length cuvette placed in the UV-Vis spectrophotometer and the amount of light transmitted was monitored over a time period of 2 hours. As the solutions were allowed to stand overnight to reach the steady state of aggregation, it was assumed that no aggregation is taking place during the time of measurement allowing sedimentation to be totally attributed to the gravitational setting depending on particle size.

A calibration study was conducted in order to see whether there is a linear relationship between the scattered light and suspension concentrations at 378 nm. For this ZnO suspensions were prepared in the range of 0.1 - 2.5 g/L by mixing ZnO nanoparticles in pH 7.5 solution and leaving overnight to achieve the equilibrium aggregate sizes.

2.7 Role of ionic strength in dissolution and aggregation

In addition to these main studies another study was conducted to see the effect of ionic strength towards dissolution and aggregation. Sodium chloride (NaCl) was used to adjust the ionic strength and same conditions were maintained at pH 7.5. Solutions were prepared by adding NaCl having concentrations in the range 0 – 500 mM. Dissolution measurements were obtained using ICP-OE spectroscopy and aggregation measurements were obtained by UV-Vis spectrometry.

CHAPTER 3

RESULTS AND DISCUSSION

3.1 Nanoparticle characterization

A summary of the characterization of the ZnO samples used in this study are given in Table 3.1. These data include average particle diameters, with standard deviation as measured from the analysis of over one hundred particles with TEM, and measured BET surface areas, triplicate measurements with standard deviations reported.

Table 3.1: Characterization data; Diameter (d) and BET surface area of ZnO nanoparticles

Diameter (nm)	BET surface area (m^2/g)
4 ± 2	105 ± 13
7 ± 2	75 ± 4
15 ± 4	47 ± 1
17 ± 3	50 ± 3
24 ± 3	40 ± 2
47 ± 7	26 ± 1
130 ± 21	11 ± 1

XRD data presented in Figure 3.1 show that these samples are crystalline and confirm expected wurtzite crystal structure for the ZnO. Peak broadening with decreasing size can be seen in XRD patterns. As a result of decrease in size a non-uniform stress is introduced to the structure which leads to the peak broadening mentioned above.

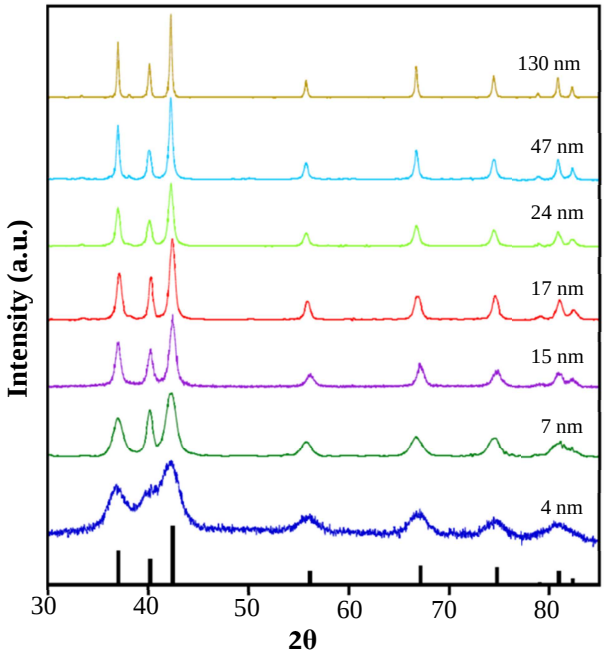

Figure 3.1: X-ray diffraction (XRD) patterns for ZnO nanoparticles of different sizes. These data show the wurtzite structure for samples used in this study.

TEM images of the ZnO samples are shown in Figure 3.2 and most of the ZnO nanoparticles are spherical in shape.

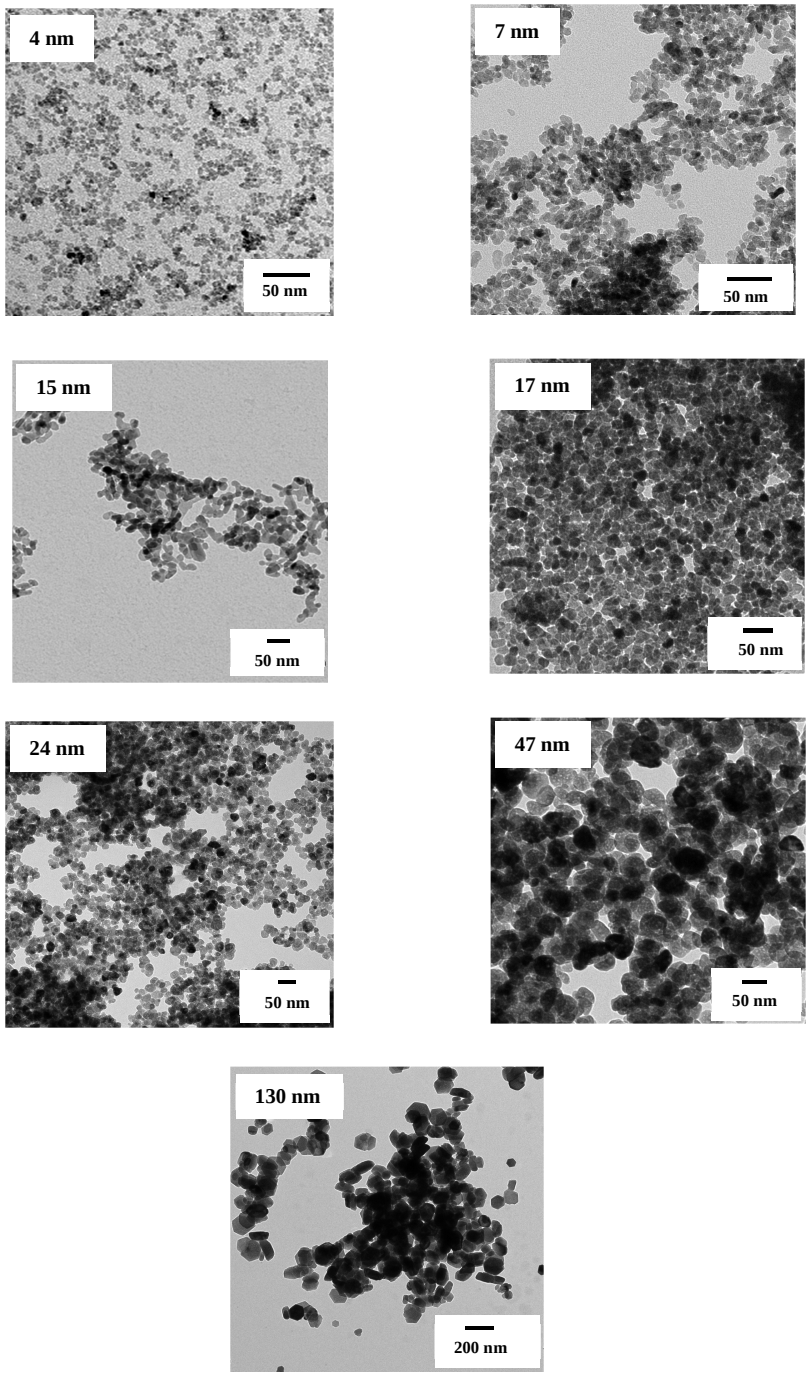

Figure 3.2 Transmission electron microscopic (TEM) images of ZnO samples

Surface functionality for these different samples was obtained from ATR-FTIR spectroscopy. These data are shown in Figure 3.3 where 4, 7 nm samples were laboratory synthesized from zinc acetate precursor whereas the 15 nm sample was purchased from Alfa Aesar.

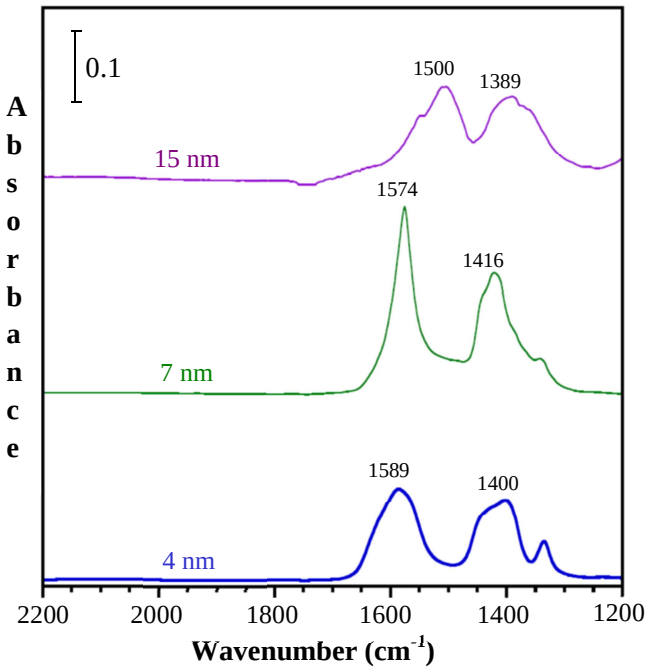

Figure 3.3: ATR-FTIR spectra for 4, 7 and 15 nm nanoparticles used in this study.

Surface adsorbed acetate groups, which originate from the zinc acetate precursor used in the synthesis, can be seen in the surface spectra of 4 and 7 nm ZnO nanoparticles. Absorption bands present at 1400 and 1589 cm^{-1} in the 4 nm ZnO surface spectrum can be assigned as symmetric and asymmetric stretching modes of COO-.[54] Two peaks

appear in 7 nm surface spectra at 1416 and 1574 cm^{-1} are also close to those observed for symmetric and asymmetric stretching modes of COO- respectively. In comparison, surface spectra of the 15 nm ZnO sample has its peaks in this region that are centered near 1389 and 1500 cm^{-1}. The frequencies of these vibrational bands are more closely associated with adsorbed carbonate groups.

3.2 Dissolution studies

3.2.1 Size dependent dissolution

Dissolution of ZnO nanoparticles (NPs) was studied using a range of size, including six laboratory synthesized ZnO samples and one commercial sample at pH 7.5. Dissolution measurements were obtained after 24 hours in order to assure aggregation and dissolution were at a steady state. However, as can be seen from the results of kinetic measurements, the amount of dissolved Zn^{2+} reaches steady state within ca. 6 hours (Figure 3.4).

Generally higher surface area can result in a higher reaction rate. However, observed higher rate of dissolution of 4 nm nanoparticles can be attributed not only to the high surface area of smaller particles but also to the reactivity of smaller nanoparticles due to the presence of surface nanoscale topographic features such as larger fraction of atoms at the edges and corners.[4] The final pH of the solutions were recorded where the final pH was raised to values ranging from 7.56 to 7.58.

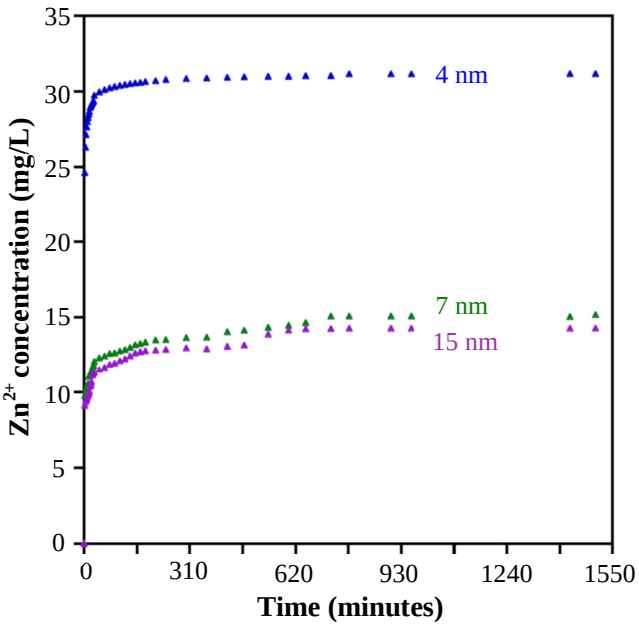

Figure 3.4: Time dependent dissolution of ZnO nanoparticles of sizes 4, 7 and 15 nm

Zinc oxide dissolution is well known and occurs over a wide range of pHs.[13] At circumneutral pH of 7.5, the dissolution of zinc oxide is small and thus a good pH to investigate size-dependent behavior due to the fact there is minimal interference from products that can form and a change in pH that occurs when large quantities dissolve. For ZnO, the following reactions are important in water at pH 7.5.[31,32]

$$ZnO\ (s) + H_2O\ (l) \rightleftharpoons Zn(OH)_2\ (s) \quad (3)$$

$$Zn(OH)_2\ (s) \rightleftharpoons Zn(OH)^+\ (aq) + OH^-\ (aq) \quad (4)$$

$$Zn(OH)^+\ (aq) \rightleftharpoons Zn^{2+}\ (aq) + OH^-\ (aq) \quad (5)$$

Overall the net reaction for the dissolution of ZnO is as follows.

$$ZnO\ (s) \rightleftharpoons Zn^{2+}\ (aq) + OH^{-}\ (aq) \qquad (6)$$

Solubility product for the dissolution of ZnO can be written in terms of Zn^{2+} and OH^- concentrations as shown below.

$$K_{sp} = [Zn^{2+}]\,[OH^-]^2 \qquad (7)$$

In the current study, the solubility product constant; K_{sp} for the samples were calculated using Zn^{2+} concentration obtained from ICP-OES analysis and the OH^- concentrations obtained via measuring the solution pH both after 24 hours. The solubility; S of ZnO is then related to K_{sp} according to equation 8.

$$S = \left[\frac{K_{sp}}{4}\right]^{\frac{1}{3}} \qquad (8)$$

Measured Zn^{2+} concentrations, equillibrium solution pH and calculated K_{sp} (Eq 7) for all seven ZnO samples are given in Table 3.2. Measured Zn^{2+} concentrations show that ZnO nanoparticles dissolve at pH 7.5 and the extent of dissolution increases with decreasing particle size. The data presented in Figure 3.5 indicate larger concentrations of Zn^{2+} and thus enhanced dissolution for the smaller ZnO nanoparticles compared to larger particles.

Table 3.2: Quantitative measurements of Zn^{2+} and pH along with calculated solubility products (K_{sp}) for ZnO nanoparticles.

Diameter (d) (nm)	$[Zn^{2+}]$ mg/L	pH	K_{sp} $(mol/L)^3$
4 ± 2	32 ± 1	7.56 ± 0.01	$(6.28 \pm 0.30)x10^{-17}$
7 ± 2	15 ± 1	7.58 ± 0.01	$(3.31 \pm 0.26)x10^{-17}$
15 ± 4	14 ± 1	7.58 ± 0.01	$(3.05 \pm 0.23)x10^{-17}$
17 ± 3	12 ± 1	7.56 ± 0.01	$(2.36 \pm 0.14)x10^{-17}$
24 ± 3	10 ± 1	7.58 ± 0.01	$(2.17 \pm 0.12)x10^{-17}$
47 ± 7	9 ± 1	7.57 ± 0.01	$(1.97 \pm 0.19)x10^{-17}$
130 ± 21	6 ± 1	7.55 ± 0.01	$(1.09 \pm 0.10)x10^{-17}$

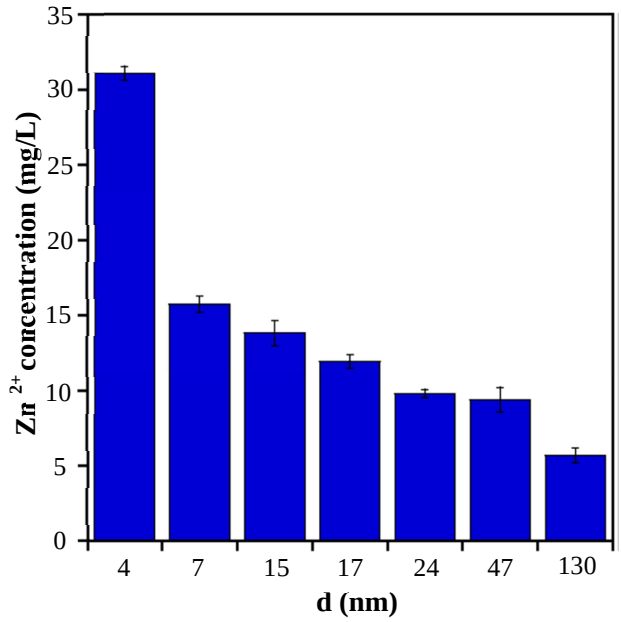

Figure 3.5: Measured Zn^{2+} concentrations after 24 hours from aqueous suspensions of ZnO nanoparticles (0.5 g/L) of different size at an initial pH of 7.5.

The above observations can be attributed to the higher surface free energy and activity of nanoparticles due to their small size in addition to the increased surface area.

The relationship between particle size and solubility can be described using the modified Kelvin equation, which is typically used to describe the change in vapor pressure due to a curved liquid-vapor interface, and is also known as Ostwald-Friedrich equation (Equation 9)[4,21,28] Accordingly, the solubility is expected to increase exponentially with decreasing particle size as follows:

$$\frac{S}{S(bulk)} = \exp\left(\frac{4\gamma V}{RTd}\right) \qquad (9)$$

where S is the solubility (in mol/kg) of a spherical particle with diameter d (m), S(bulk) is the solubility of the bulk, γ is the surface free energy (in mJ/m^2), V is the molecular volume (in m^3/mol), R is the gas constant (in mJ/mol K) and T is the temperature (in K). As size decreases, the surface energy of the particles is expected to increase which result in enhanced dissolution.[4]

This equation can be related to the solubility product constant (equation 7) and linearized to give,

$$\ln K_{sp} = \ln K_{sp}^{bulk} + \frac{12\gamma V}{RTd} \qquad (10)$$

As can be seen from equation 10, assuming a constant V and γ with varying size, a plot of ln K_{sp} vs d^{-1} can be used to deduce both the surface energy and the bulk solubility product constant of the ZnO nanoparticles. Using the solubility product constant values in Table 4, ln K_{sp} vs d^{-1} for all seven ZnO samples is plotted in Figure 3.6.

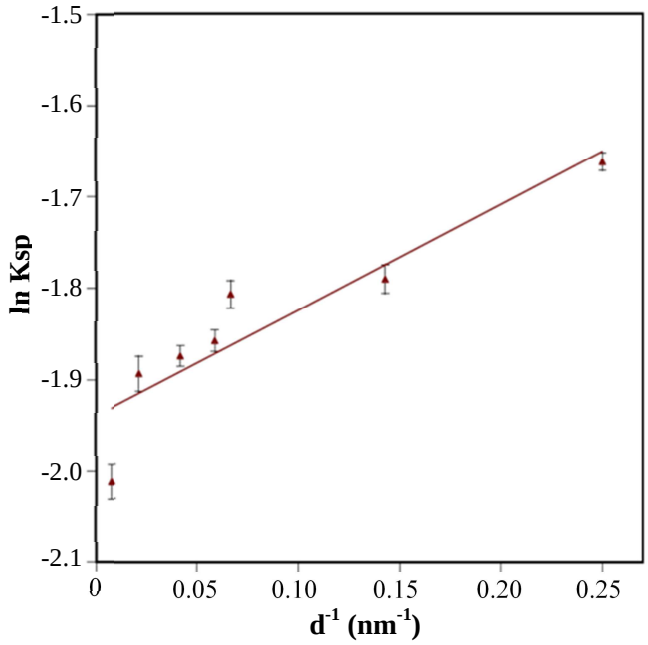

Figure 3.6: Variation of ln K_{sp} with d^{-1} using experimental K_{sp} values for different ZnO samples

Experimental results are qualitatively in agreement with the theoretical prediction depicted by the linearized Kelvin equation (equation 10). But quantitatively several deviations were observed. The bulk solubility product constant ($1.6x10^{-17}$ mol^3/L^3) obtained from Figure 3.6 was comparable to the $1.7x10^{-17}$ mol^3/L^3 stated in the literature However, the bulk solubility (0.14 mg/L) obtained from this study significantly differed from the bulk value of 1.6 mg/L at pH 7.0 stated in the literature. This may be due to the higher equilibrium pH recorded in the current study. According to literature a transition condition in which the solubility varies steeply with the pH for wurtzite – ZnO (20 – 100 nm) exists for pH ranges 6.0 – 9.0 and 11.5 – 13.0.[32]

Furthermore, the surface energy calculated using the slope of ln S(d) vs d^{-1} plot was 0.08 J/m^2. This was smaller than the expected value stated in literature for metal oxide nanoparticles in solution which is in the range of 0.1 - 0.5 J/m^2.[37] However, there are different values reported for the surface energy of ZnO nanoparticles. For example, according to Zhang *et. al.* the value was 1.31 and 2.55 J/m^2 for hydrous and anhydrous surfaces respectively which is then fifteen to forty times greater than that was measured.[35]

These variations can originate from different surface functional groups introduced on the surface based on the synthetic procedure. Surface adsorbed species are known to reduce the surface energy considerably and is clearly seen by the difference in the values for hydrous and anhydrous surfaces discussed above. In the current study, the characterization data showed the presence of surface adsorbed acetate groups (Figure 3.3) which could potentially contribute towards lowering the surface energy. Furthermore, the surface energy calculated is an average of the surface crystal faces. This average value may or may not be representative of all the planes. Park *et. al.* has shown that for three dimensional assemblies of TiO_2 the average surface energy is closer to that of simple TiO_2 nanoparticle structures with (101) dominant surface planes whereas ZnO tetrapods showed larger deviations in the average surface energy.[55] Thus the surface crystal planes of the ZnO samples used in the current study may differ from those discussed in literature.

Another key factor contributing towards the lowered surface energy obtained can result from aggregation as can be seen by the large hydrodynamic diameters observed (Table 3.3). Therefore, deviation of the calculated surface energy in the current study

from that of literature may arise as a result of lowered surface energy by surface adsorbed groups, differences in the surface crystal planes and aggregation in the solution.

Table 3.3: Hydrodynamic diameter of ZnO nanoparticles after 24 hours at pH 7.5

Diameter (d) (nm)	Hydrodynamic diameter (nm)
4 ± 1	3409 ± 300
7 ± 2	1737 ± 63
15 ± 4	2712 ± 112
17 ± 3	2151 ± 143
24 ± 3	1897 ± 93
47 ± 7	2726 ± 400
130 ± 21	2150 ± 300

Apart from the differences in the actual experimental conditions, differences between the samples and synthesis procedures, the theoretical model itself has some drawbacks. Although it has been assumed in modified Kelvin equation that the nanoparticles are spherical, not all nanoparticles have the same spherical shape.[21,28] Thus, the faceted structures with diverse shapes can lead to the deviations.

In addition aggregation leads to formation of several irregularly shaped structures such that the actual size of particles becomes uncertain. Aggregation has been shown to decrease the rate of dissolution and even completely quench the process in some cases.[4,53] It is postulated that effective, reactive surface area of the nanoparticles exposed to the solution is reduced due to aggregation and the solution properties within the aggregates are different from the bulk. Aggregation plays a significant role in dissolution of nanoparticles and is not accounted for in the modified Kelvin equation.[4,56]

Furthermore, deviations can be expected due to the lack of detailed knowledge of the surface free energy, γ. Different surface energies has been successfully correlated with different morphologies of nanomaterials which clearly indicate the dependence of surface energy on the exposed crystal planes.[35,55] Also ZnO nanoparticles with different sizes do not have the same number of edge and corner atoms.[57] Therefore their surface to volume ratio is different and hence their surface free energies are different.

Additionally most stable crystal planes of nanoparticles vary with size. Modified Kelvin equation does not account for these potential size dependencies of γ and also for its dependence on surface properties such as defects and different surface crystal facets.[4] It has been revealed from several research studies that one of the major problems associated with the modified Kelvin equation is the uncertainty as to whether the value of γ is constant for very small particles.[28,58]

Size dependent dissolution of nanoparticles is a controversial topic in the current research where some claims its prevalence whereas the others do not. For ZnO nanoparticle suspensions, which are considered to be dynamic systems with changing suspension properties such as pH, and ionic strength, size dependent dissolution still

remains an unanswered question. For example, Meulenkamp extensively discusses the size selective etching of ZnO nanoparticles by anhydrous acetic acid in ethanolic solution and the results show that for a mixture of 3.15 nm and 4.30 nm ZnO nanoparticles the former etches at a much faster rate.[22] However, based on particle size evolution during the etching process it was clearly shown that particle size decrease is much smaller than predicted using a simple model of cube-root dependence where all the surface particles detach at the same rate. However, the experimental particle size evolution was successfully simulated in a Monte Carlo process where size-dependence and polydispersity had been accounted for. Another study on acidic dissolution of single – crystalline ZnO (0001) surfaces by in-situ AFM imaging showed that for pH 5.5 – 3.8, the dissolution precede only along the pre-existing edges and not along the terraces.[59] This was successfully correlated to the positively charged surface at this pH for the (0001) terraces inhibiting the proton promoted dissolution in contrast to the other crystallographic planes (1120 or 1010) present at the edges. In a different study on the dissolution of PbS nanocrystals, greater dissolution for (110) and (111) edges were exhibited over (100) primary terraces as shown by the HRTEM images.[56] Furthermore, comparison of the dissolution rates of 14.4 nm PbS nanocrystals vs 3.1 μm crystals gave 10 times greater rate for the former than the latter.[4] Peng *et. al.* on the other hand indicate no observed size dependent dissolution of ZnO nanoparticles in marine water.[36]

3.2.2 Effect of complexing ligands on the dissolution of ZnO nanoparticles

As discussed in Section 3.2.1, a size dependent dissolution was clearly observed even in the presence of aggregation for ZnO nanoparticles at circumneutral pH. However, it is important to highlight that this observation was achieved with a simple matrix. The observed size dependence gets masked completely upon addition of citric acid to the medium and a higher degree of dissolution also was observed.

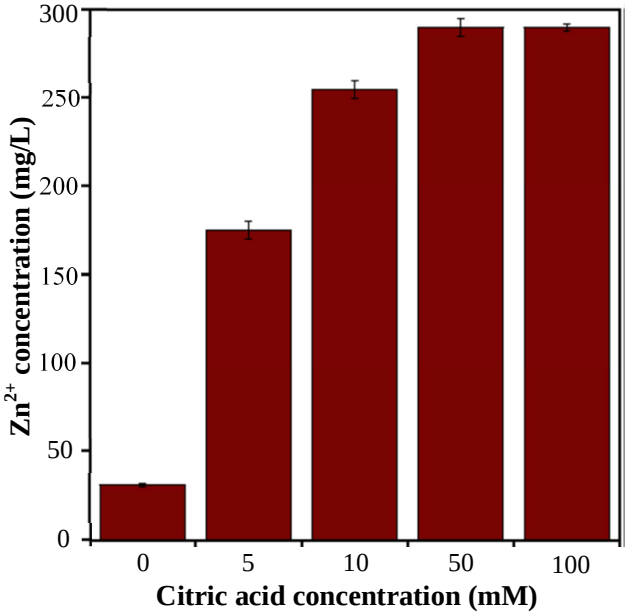

Figure 3.7: Dissolution of 4 nm ZnO in the presence of citric acid after 24 hours as a function of citric acid concentration.

Citric acid with its multiple carboxylate groups is a good complexing ligand.[30] The objective of using citric acid in the current study was to investigate the effect the complexing ligands on dissolution of nanoparticles.

The presence of citric acid clearly affected the dissolution process as can be seen by increasing dissolution as a function of citric acid concentration (Figure 3.7) for 4 nm ZnO nanoprticles. The maximum dissolution was obtained at citric acid concentrations ≥ 50 mM. This is approximately a 10 fold increase compared to the absence of citric acid. Since citrate is a polydentate ligand it can form strong coordinating complexes with the surface of oxide nanoparticles. This can lead to a higher degree of dissolution associated with the detachment of metal cations from the surface. Formation of this complex between the metal cation and the ligand weakens the metal oxide bond eventually leading to higher extent of detachment which results in a higher degree of dissolution.

Using 50 mM concentration to ensure that dissolution is not limited by available citric acid, the dissolution experiments of ZnO were conducted for 4, 7, 15, 17, 24 and 47 nm samples. As can be seen in figure 3.8, approximately the same degree of dissolution was observed irrespective of the size. However, a significant increase in solution pH was observed (final pH in the range of 8.36 - 8.76) after 24 hours in the presence of citric acid.

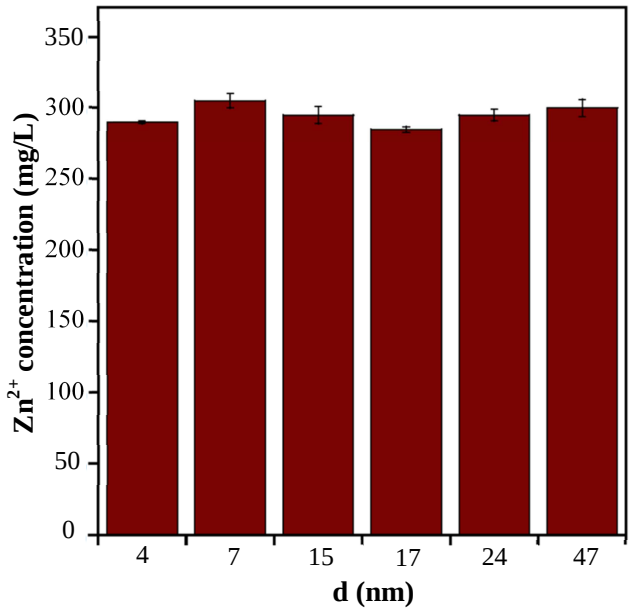

Figure 3.8: Dissolution of ZnO in the presence of 50 mM citric acid at pH 7.5 (initial) as a function of size.

This contradicting observation obtained from the matrices with different complexities highlight several important points. Size dependent dissolution does exist for ZnO nanoparticles as shown in Figure 3.5. As the size of the particles decrease surface area and the number of edges, kinks and defect site density increase creating “hot spots” of dissolution. Thus enhanced dissolution properties are observed for smaller particles. However, when complexing ligands are present in the medium, these can adsorb on to the majority of flat terraces polarizing and weakening the metal-oxygen bonds of the lattice surface. Thus in the presence of such ligands, additional dissolution hot spots are created on the terraces other than the edges and kinks leading to same extent of dissolution for

both nanoscale and bulk materials explaining the masking of size dependent dissolution (Figure 3.8).

3.3 Adsorption of complexing agents onto ZnO surface

Adsorption of citrate onto ZnO surface was studied for samples of sizes 4, 7 and 15 nm. Solution phase spectrum for citric acid (100mM) also was obtained and shown in Figure 3.9. According to Figure 1.3 b, citric acid is fully deprotonated at pH 7.5 and has prominent absorption bands at 1569, 1388 and relatively week band at 1280 cm^{-1}(Figure 3.9).

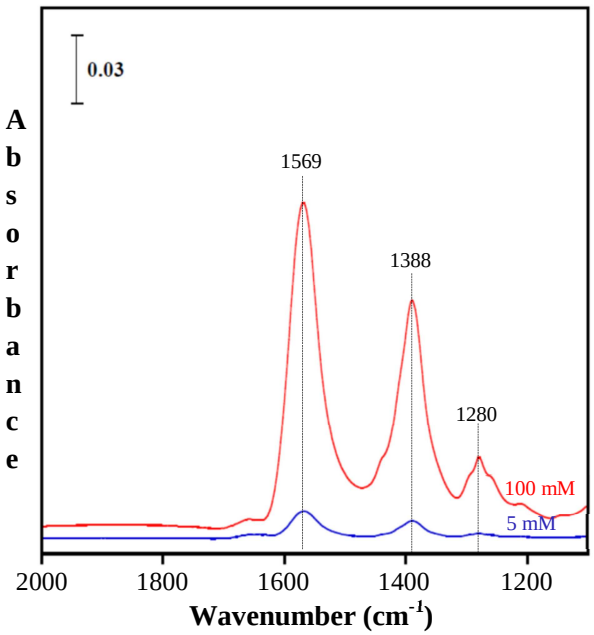

Figure 3.9: ATR-FTIR spectra for 5,100 mM citric acid in solution phase at pH 7.5

Observed peaks were assigned to different vibrational peaks and presented in Table 3.4.

Table 3.4: Assigned vibration modes of citric acid at pH 7.5 and comparison with the literature values.

Vibration mode	Experimental value (cm^{-1})	Theoretical value[60] (cm^{-1})
ν_{as} (COO^-)	1569	1572
δ (CH_2)	1438	1438
ν_s (COO^-)	1388	1389
δ (O=C-O^-)	1280	1278
ν (C-OH)	1094	1100

Two prominent bands at 1569 and 1388 cm^{-1} can be assigned to the asymmetric and symmetric stretching modes of carboxylic group respectively. This is in good agreement with the literature values as shown in Table 3.4. Furthermore, weak band at 1280 cm^{-1} was assigned to coupled stretches and bends of carboxylic group.[30] Collected solution phase spectrum for 5 mM citric acid at pH 7.5 is also shown in Figure 3.9. Compared to 100 mM, this has a lower intensity as a consequence of lower concentration.

ATR-FTIR spectra of surface adsorbed citrates were obtained over a period of 2 hours and shown in Figure 3.10.

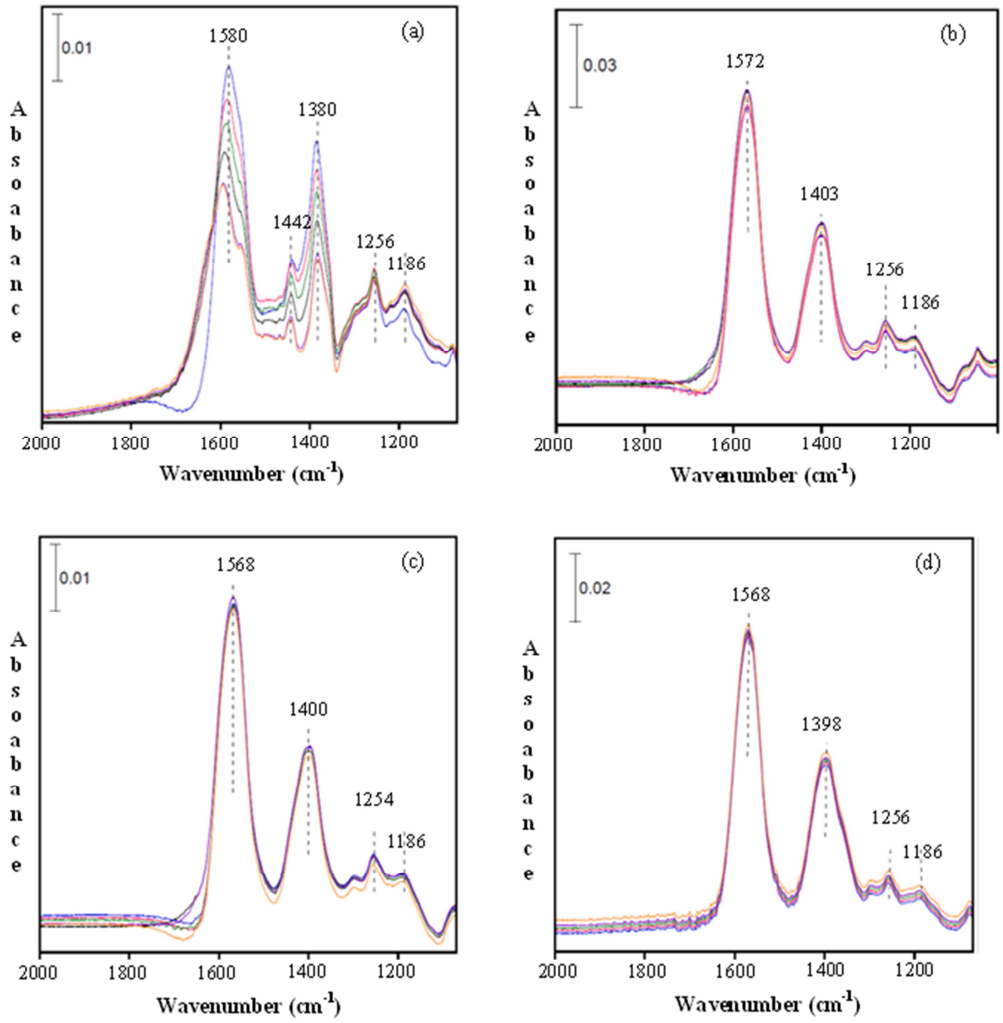

Figure 3.10: ATR-FTIR spectra of surface adsorbed citric acid for (a) 4 nm (b) 7nm (c) 15 nm (d) 30 nm samples.

Spectra shown in Figure 3.10 were collected in the presence of 5 mM citric acid and as mentioned earlier, very weak spectra were obtained for citric acid concentrations less than 100 mM. However, intense spectra obtained in the presence of ZnO thin film even for low concentrations of citric acid can be attributed to the adsorption of citrates onto the surface of ZnO nanoparticles. Thin film of ZnO nanoparticles has a large number of surface adsorption sites and upon adsorption, concentration of citrate molecules on the surface increases eventually resulting in a higher concentration of surface adsorbed citrates. Because of this, an intense spectrum is observed.

ATR-FTIR spectra for surface adsorbed citrates appear similar to the solution phase. However absorption bands for the surface adsorbed species looked broader compared to the solution phase and the peak intensity of absorption bands were decreased with time. This can be explained by the dissolution of ZnO nanoparticles where number of available adsorption sites decrease upon dissolution.

3.4 Zeta potential measurements

Surface charge of ZnO nanoparticles were measured in the presence as well as in the absence of citric acid using zeta potential measurements. In general zeta potential measurements specifies the electrokinetic potential of a colloidal system.[61] This is a physical property which is exhibited by any particle in a suspension. Magnitude of the zeta potential gives the net charge at the diffuse boundary of a particle in a suspension which will ultimately indicate the potential stability of a colloidal system.[62]

If the particles in a suspension have large negative or positive zeta potential values, particles will repel each other and there will be no aggregation of nanoparticles. On the other hand, if particles have small zeta potential values there is no force to prevent particle coming together and their aggregation. It is generally considered that the zeta potential values greater than +30 mV or smaller than -30 mV, result in stable suspensions.[61,62] However these values can slightly change depending on several factors such as density and pH.

Point of zero charge (pH_{PZC}) for the ZnO samples of sizes 4, 7 and 15 nm were also obtained from zeta potential experiments. Generally, pH_{PZC} is the point at which the net electrical charge density on a surface is zero.[63] This is generally determined in relation to the pH of the medium and therefore it is also called as the pH at which the surface of a particle shows no net charge.[64] In order to determine pH_{PZC}, a series of suspensions of ZnO were prepared at different pH values and the zeta potentials were measured.

Figure 3.11 shows the variation of zeta potential with pH for 4 nm ZnO sample. pH_{PZC} , the pH at which zeta potential is zero is shown in red. This was obtained by linear extrapolation between pH 8 and 10 and the value (8.75) is in agreement with the literature value which is in the range of 8.5- 9.0 for Zno nanoparticles.[34] When pH of the medium is below this pH (8.75), ZnO surface is positively charged. Below the pH_{PZC}, acidic water donates more H^+ ions than OH^- , so that the surface of adsorbent gets positively charged. Conversely, above this pH surface is negatively charged as a result of dominant OH^- ions.

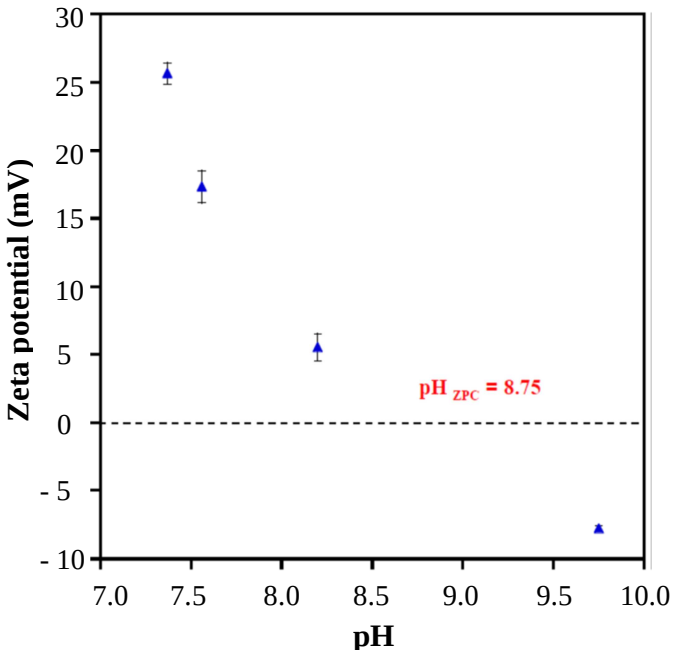

Figure 3.11: Variation of surface charge with pH for 4 nm ZnO sample. pH_{ZPC} is shown in red.

pH_{PZC} for 7 and 15 nm samples were also obtained by plotting zeta potential vs pH followed by linear extrapolation. Observed values were 8.48 and 8.63 respectively.

Surface charge of ZnO samples were measured in the absence of citric acid and with increasing citric acid concentration (0.3 - 5.0 mM). Observed surface charges are shown in Table 3.5 and variation of surface charge with increasing citric acid concentration for 4 nm sample is graphically represented in Figure 3.12. According to data, in the absence of citric acid ZnO surface is positively charged and this is in

agreement with the theoretical prediction for a surface below its pH $_{ZPC}$, where the measurements were made at pH 7.5 which is below pH $_{ZPC}$ of 4 nm ZnO nanoparticles. Observed value being less than 30 mV suggests that aggregation can take place. A negative charge has been developed on the surface upon addition of citric acid reaching larger negative surface charge (-50 mV) in the presence of 5 mM citric acid.

Table 3.5: Surface charge of ZnO samples of sizes 4, 7 and 15 nm with varying citric acid concentrations at initial pH of 7.5

	Citric acid concentration (mM)			
Sample no	0 Zeta potential (mV)	0.3 Zeta potential (mV)	1.0 Zeta potential (mV)	5.0 Zeta potential (mV)
4 nm	+ 20.7	-19.1	- 44.2	- 49.7
7 nm	+ 20.4	- 18.0	- 23.0	- 36.4
15 nm	+ 15.6	- 9.9	- 28.3	- 40.2

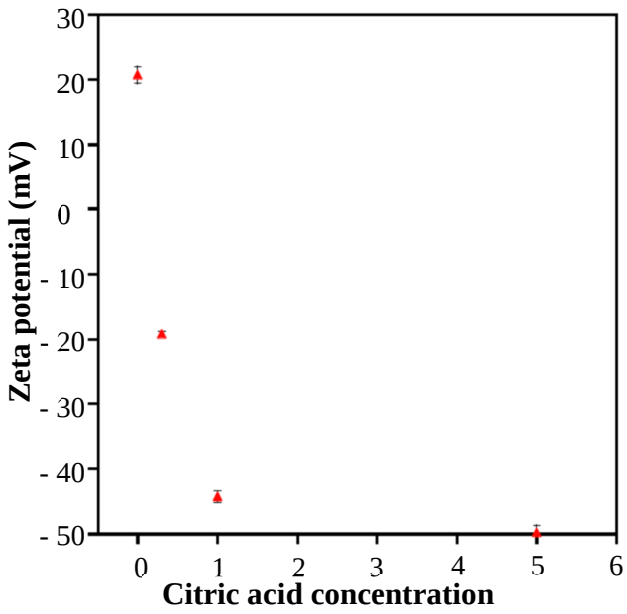

Figure 3.12: Variation of surface charge with increasing citric acid concentration for 4 nm ZnO sample

Dominant form of citric acid at this pH is Cit^{3-} and once it is adsorbed onto the surface, a negative charge is generated as shown in Figure 3.13.

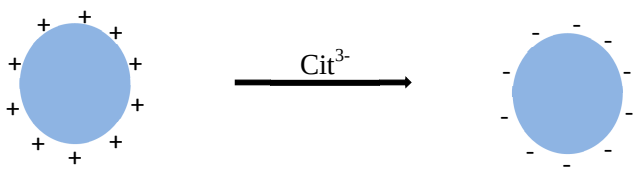

Figure 3.13: Schematic representation of the formation of negative charge

Formation of a stable suspension was observed in the presence of 5 mM citric acid. Surface charge being smaller than -30 mV suggests that aggregation will not take place as a result of repulsive forces between highly negative charged surfaces. As a result a stable suspension can be formed and this will be further discussed under aggregation studies.

3.5 Aggregation studies

Stability of ZnO nanoparticles were studied in the presence as well as in the absence of citric acid. In this study, quantitative techniques such as DLS and qualitative techniques such as sedimentation plots were used to study the aggregation of ZnO nanoparticles.

3.5.1 Quantitative measurements- DLS technique

Hydrodynamic diameter of ZnO nanoparticles after 24 hours were measured in the absence of citric acid and shown in Table 5. According to DLS data, aggregation readily occurs and particles are in the range of 1-3 µm. In order to reduce their high surface energy, nanoparticles tend to attract each other forming larger aggregates.

Same experiments were done in the presence of citric acid (0.3 – 5.0 mM) and the results are graphically presented in Figure 3.14. As can be seen, hydrodynamic diameter has been decreased with increasing citric acid concentration. Decrease in particle size suggests that less aggregation occurs in the presence of citric acid.

As mentioned earlier, at pH 7.5, citric acid is fully deprotonated where Cit^{3-} is the dominant species and this can adsorb onto ZnO nanoparticles making the surface negatively charged. Development of a negative charge on ZnO surface results in a repulsion between ZnO nanoparticles. This eventually leads to a lesser degree of aggregation. Development of the negative charge on surface was discussed under section 3.4.

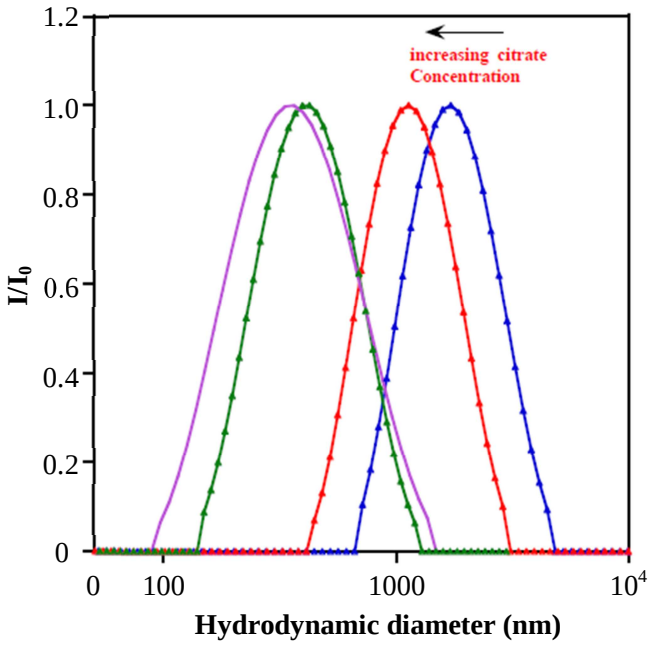

Figure 3.14: Intensity normalized aggregate size distribution of 4 nm ZnO sample with changing citric acid concentration.

3.5.2 Qualitative measurements – Sedimentation experiments

Sedimentation experiments were conducted with a UV-Vis spectrophotometer in order to study the aggregation pattern in the presence and absence of citric acid.

Linear relationship was observed between scattered light and suspension concentrations at 378 nm in the range 0.1 – 2.5 g/L. Observed calibration plot is shown in Figure 3.15.

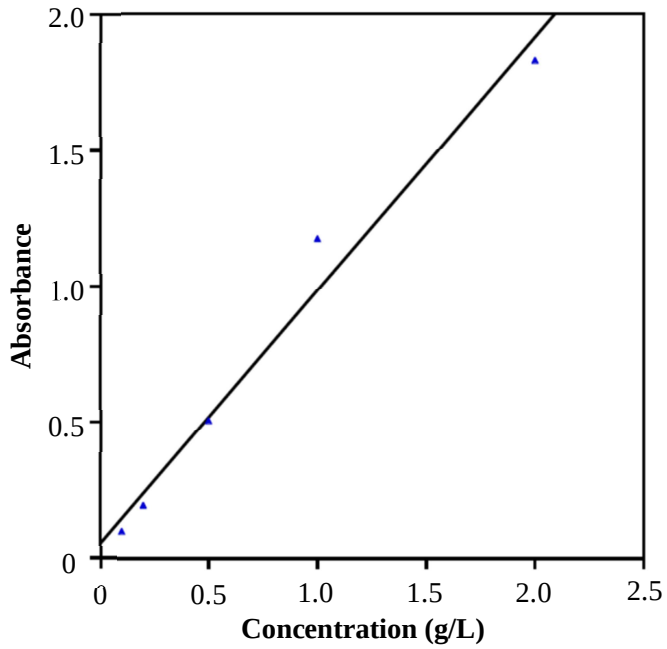

Figure 3.15: Calibration plot for ZnO sedimentation (pH 7.5) measured at 378 nm. A linear relationship was observed with a R^2 value of 0.99.

A solid loading of 0.5 g/L which is in the linear range was selected for further experiments. Sedimentation plots as a function of time are shown in Figure 3.16.

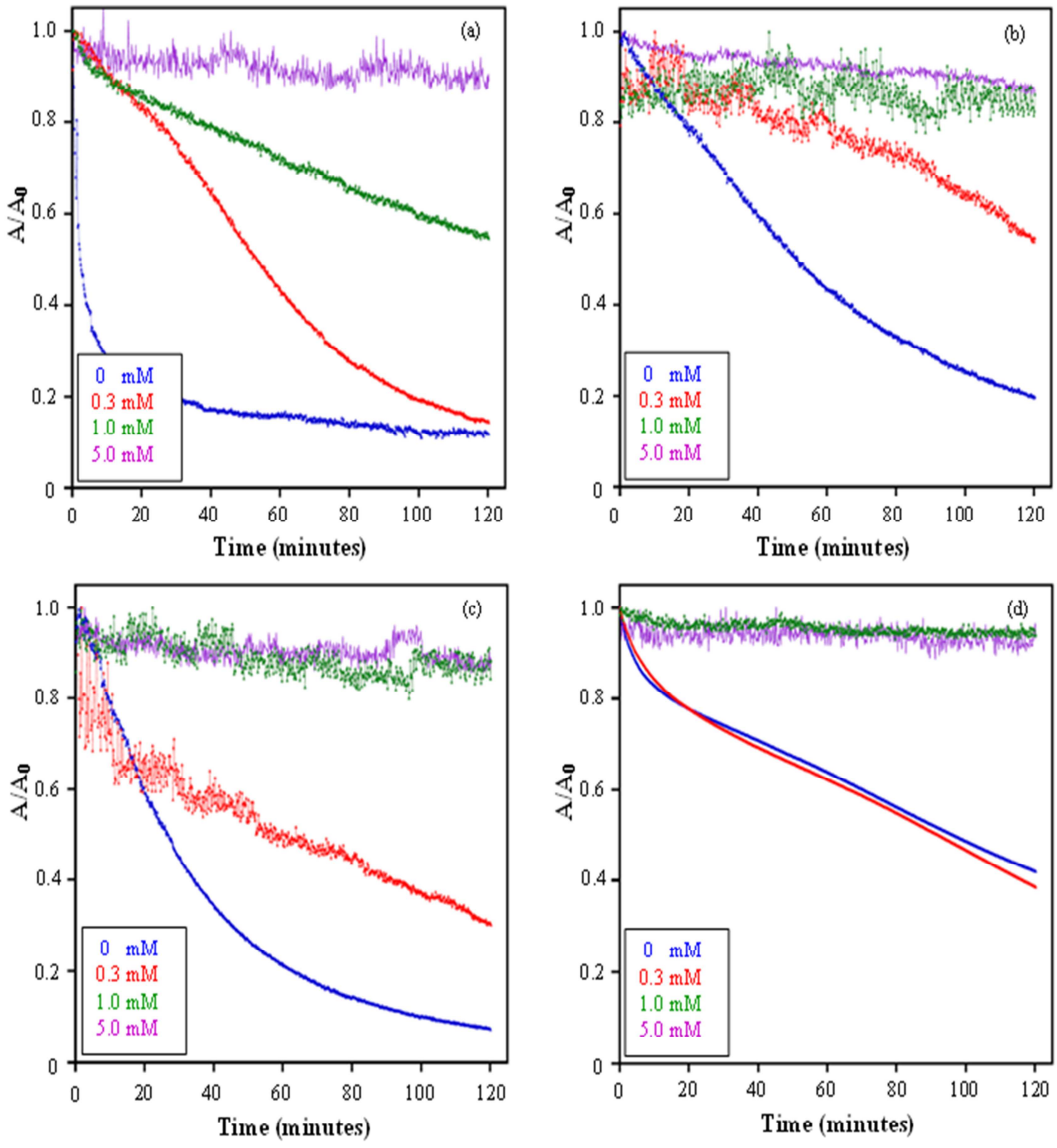

Figure 3.16: Sedimentation of ZnO with increasing citric acid concentration as a function of time at pH 7.5. (a) 4nm (b) 7 nm (c) 15 nm (d) 30 nm

These data suggests that Zno nanoparticles settle out of solution as a function of time. In the absence of citric acid higher sedimentation rate was observed for all the samples suggesting a higher degree of aggregation. This observation is in agreement with DLS data and zeta potential measurement shown earlier.

However, sedimentation rate has gradually been decreased with increasing citric acid concentration. In the presence of 5 mM citric acid sedimentation rate is almost zero resulting in a stable suspension. Aggregation pattern of ZnO nanoparticles and their interaction with each other alters in the presence and absence of citric acid at circumneutral pH where citric acid stabilizes ZnO nanoparticles.

This observed reversal of suspension stabilities in the presence of organic acids is again attributed to the adsorption of citrate anion onto the surface of ZnO nanoparticles as described earlier. Adsorbed citrate develops a negative charge on the surface resulting in a double layer formation eventually decreasing nanoparticle aggregation. Over all, sedimentation, DLS and zeta potential measurements are in agreement with each other supporting this conclusion.

Aggregation is an important key factor in determining the distribution of nanoparticles in the environment. As observed in this study, various compounds can alter the aggregation pattern of ENPs resulting in different extents their of bio availability. Larger aggregates tend to settle down rapidly and this will limit their availability in the aquatic system and air. But aggregates will remain in soil or colloids.

It has been observed in several other studies that aggregation is hampered in the presence of natural organic matter (NOM). A study by Zhou *et.al* has shown that aggregation of ZnO nanoparticles is effectively hindered in the presence of NOM.[34]

Domingos *et.al* has pointed out that fulvic acid can stabilize TiO_2 nanoparticles due to increased steric repulsion.[65] A study on adsorption of citric acid onto TiO_2 nanoparticles by Mudunkotuwa *et.al* has observed a reversal of suspension stabilities with varying pH.[30] Conversely, in another study Bian *et.al* has observed a higher sedimentation rate in the presence of humic acid.[13] However, several other factors like ionic strength, pH and particle morphology can also affect the aggregation pattern of nanoparticles.

3.6 Role of ionic strength in dissolution and aggregation

3.6.1 Dissolution studies

Observed dissolution pattern with changing ionic strength for 4 nm sample is shown in Figure 3.17. According to data, dissolution has gradually been increased reaching a maximum in the presence of 50 mM NaCl and has remained constant irrespective of the NaCl concentration. Highest dissolution observed was 43 mg/L.

It is generally expected to increase the dissolution with increasing ionic strength and this can be explained by Debye Huckel law. However further experiments are required to understand this dissolution behavior.

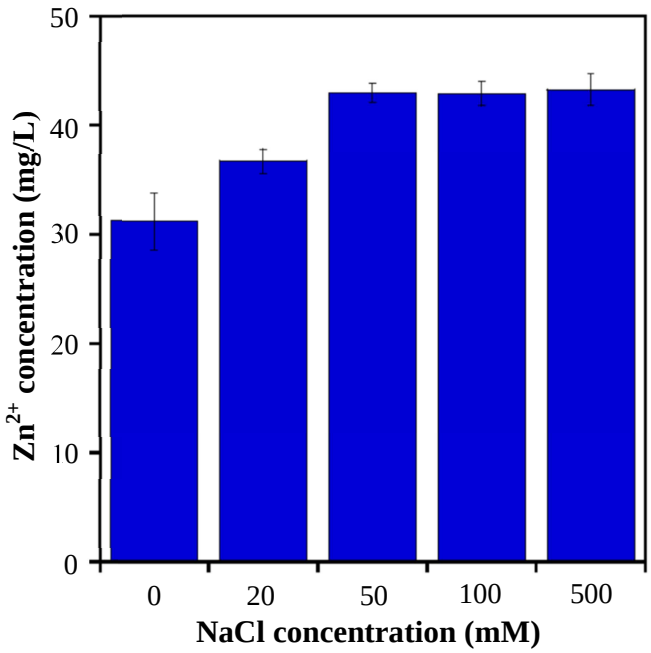

Figure 3.17: Dissolution measurements as a function of NaCl concentration at pH 7.5 for 4 nm sample.

3.6.2 Aggregation studies

Aggregation also was studied over the same range of NaCl concentration keeping all the other conditions constant. Sedimentation plots with varying ionic strength are shown in Figure 3.18 and sedimentation rate has been augmented with ionic strength as a result of increasing aggregation. Highest sedimentation rate was observed in the presence of 500 mM NaCl.

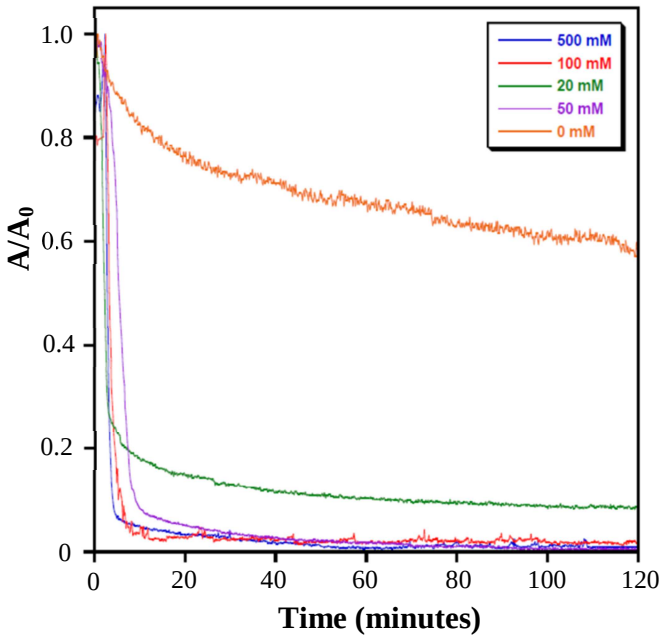

Figure 3.18: Sedimentation plots with changing ionic strength for 4 nm ZnO nanoparticles at pH 7.5

Observed higher extent of aggregation can be explained by the compression of electrical double layer in the presence of high ion content. It is generally believed that electrolytes in a colloidal system control the thickness of electric double layer (EDL). Higher ion concentration reduces the thickness of EDL. Hence electro static repulsion is decreased eventually leading to a higher degree of aggregation as observed in Figure 3.18.[34]

However hydrodynamic diameter and surface charge measurements are required before drawing a conclusion on the role of ionic strength in dissolution and aggregation.

CHAPTER 4

CONCLUSIONS

This thesis is based on two main studies. First is the story of dissolution of ZnO nanoparticles in the presence and absence of citric acid where size dependent dissolution comes in to the picture. Second is the study of the aggregation of ZnO nanoparticles in the presence and absence of citric acid. In addition, ATR-FTIR spectroscopic studies were conducted to get a better insight into the adsorption of citric acid onto ZnO nanoparticles. Furthermore, role of ionic strength in dissolution and aggregation was also studied.

A number of interesting and significant conclusions can be drawn from the results of these studies on dissolution and aggregation of well characterized ZnO nanoparticles in the presence of organic acids. According to first study, smaller nanoparticles show a greater extent of dissolution compared to larger particles as expected from classical theoretical predictions depicted by the modified Kelvin equation and particle size. Second, there are quantitative deviations from the modified Kelvin equation which can arise from the presence of surface functional groups, dependence of γ on exposed crystal planes and aggregation. Third, the theoretical model itself lacks detailed surface topographic parameters to achieve accurate quantitative predictions. Finally a higher extent of dissolution was observed in the presence of citric acid and the size dependent dissolution of ZnO was completely masked in the presence of citric acid which was attributed to the ligand promoted dissolution.

According to second study, aggregation readily occurs in the solution in the absence of citric acid. Nanoparticle aggregation plays a significant role in dissolution and here it is shown that ZnO nanoparticles aggregated to larger size micron particles under the condition of these studies. However, the aggregation did not completely mask the size dependent dissolution of ZnO as commonly suggested. Secondly, adsorption of citrates onto ZnO nanoparticles was observed using ATR-FTIR spectroscopy. Third, a reversal of surface charge of ZnO nanoparticles was observed upon adsorption of citrates. At current pH citric acid is fully deprotonated where Cit^{3-} is the dominant species. This negatively charged species adsorb onto ZnO nanoparticles making their surfaces negatively charged and this result in repulsion between nanoparticles eventually leading to a lesser extent of aggregation. Fourth, formation of a stable suspension was observed in the presence of citric acid. This trend observed in aggregation pattern are of great environmental and biological importance as citric acid is abundant in the environment as well as in human body and as aggregation plays a significant part in determining the availability of ENPs in the environment. Finally aggregation was enhanced with increasing ionic strength as well as the dissolution. However dissolution reached a maximum after a certain concentration of electrolytes.

Overall, this study provides a link between theoretical predictions and actual experimental observations of size dependent dissolution of nanoparticles where only few such studies are available in literature with detailed discussion on both the conceptual framework with sound experimental background. In addition it also provides a better insight into the behavior of ENPs under different environmental conditions such as in the

presence of complexing agents and different salts which is very imperative in determining the fate of ENPs once they are released to the environment.

REFERENCES

(1) Nowack, B.; Bucheli, T. D. *Environmental Pollution* **2007**, 150, 5-22.

(2) Brayner, R.; Dahoumane, S. A.; YeÌ preÌ mian, C.; Djediat, C.; Meyer, M. l.; CouteÌ , A.; FieÌ vet, F. *Langmuir* **2010**, 26, 6522-6528.

(3) Zhang, H.; Chen, B.; Banfield, J. F. *The Journal of Physical Chemistry C* **2010**, 114, 14876-14884.

(4) Liu, J.; Aruguete, D. M.; Murayama, M.; Hochella, M. F. *Environmental Science & Technology* **2009**, 43, 8178-8183.

(5) Zhang, Y.; Chen, Y.; Westerhoff, P.; Hristovski, K.; Crittenden, J. C. *Water Research* **2008**, 42, 2204-2212.

(6) Petosa, A. R.; Jaisi, D. P.; Quevedo, I. R.; Elimelech, M.; Tufenkji, N. *Environmental Science & Technology* **2010**, 44, 6532-6549.

(7) Tiede, K.; Hassellöv, M.; Breitbarth, E.; Chaudhry, Q.; Boxall, A. B. A. *Journal of Chromatography A* **2009**, 1216, 503-509.

(8) Grassian, V. H. *The Journal of Physical Chemistry C* **2008**, 112, 18303-18313.

(9) Abbas, Z.; Labbez, C.; Nordholm, S.; Ahlberg, E. *The Journal of Physical Chemistry C* **2008**, 112, 5715-5723.

(10) Rao, C. N. R.; Kulkarni, G. U.; Thomas, P. J.; Edwards, P. P. *Chemistry – A European Journal* **2002**, 8, 28-35.

(11) Jolivet, J.-P.; Froidefond, C.; Pottier, A.; Chaneac, C.; Cassaignon, S.; Tronc, E.; Euzen, P. *Journal of Materials Chemistry* **2004**, 14, 3281-3288.

(12) Zhao, Q.; Xie, T.; Peng, L.; Lin, Y.; Wang, P.; Peng, L.; Wang, D. *The Journal of Physical Chemistry C* **2007**, 111, 17136-17145.

(13) Bian, S.-W.; Mudunkotuwa, I. A.; Rupasinghe, T.; Grassian, V. H. *Langmuir* **2011**, 27, 6059-6068.

(14) Joner, E. J. H., T.; Amundsen; C.E. Environmental fate and ecotoxicity of engineered nanoparticles , **2008**.

(15) French, R. A.; Jacobson, A. R.; Kim, B.; Isley, S. L.; Penn, R. L.; Baveye, P. C. *Environmental Science & Technology* **2009**, 43, 1354-1359.

(16) Cao, G. *Nanostructures and nanomaterials*; First ed.; Imperial college press: London, 2004.

(17) Ju-Nam, Y.; Lead, J. R. Science of *The Total Environment* **2008**, 400, 396-414.

(18) In Global Information, Inc. Market reports **2010**.

(19) Lowry, G. V. In EPS OSWER workshop on nanotachnology **2006**.

(20) Van Eerdenbrugh, B.; Vermant, J.; Martens, J. A.; Froyen, L.; Humbeeck, J. V.; Van den Mooter, G.; Augustijns, P. *Molecular Pharmaceutics* **2010**, 7, 1858-1870.

(21) Letellier, P. M., A.; Turmine, M. Journal of Physics: *Condensed Matter* **2007**, 19, 496229.

(22) Meulenkamp, E. A. *The Journal of Physical Chemistry B* **1998**, 102, 7764-7769.

(23) Colvin, V. L. *Nature Biotechnology* **2003**, 21, 1166.

(24) Zhang, Y.; Chen, Y.; Westerhoff, P.; Crittenden, J. *Water Research* **2009**, 43, 4249-4257.

(25) Tso, C. P.; Zhung, C. M.; Shih, Y. H.; Tseng, Y. M.; Wu, S. C.; Doong, R. A. *Water Science and Technology* **2010**, 61, 127-133.

(26) Dundon, M. L. M., E. Journal the American Chemical Socity 1923, 45, 2658.

(27) Enustun, B. V. T., J. *Journal of the American Chemical Society* **1960**, 82, 4502.

(28) Mihranyan, A.; Strømme, M. *Surface Science* **2007**, 601, 315-319.

(29) Pettibone, J. M.; Cwiertny, D. M.; Scherer, M.; Grassian, V. H. *Langmuir* **2008**, 24, 6659-6667.

(30) Mudunkotuwa, I. A.; Grassian, V. H. *Journal of the American Chemical Society* **2010**, 132, 14986-14994.

(31) Degen, A.; Kosec, M. *Journal of the European Ceramic Society* **2000**, 20, 667-673.

(32) Yamabi, S.; Imai, H. *Journal of Materials Chemistry* **2002**, 12, 3773-3778.

(33) Wang, Z. L. *Journal of Physics: Condense Matter* **2004**, 16.

(34) Zhou, D.; Keller, A. A. *Water Research* **2010**, 44, 2948-2956.

(35) Zhang, P.; Xu, F.; Navrotsky, A.; Lee, J. S.; Kim, S.; Liu, J. *Chemistry of Materials* **2007**, 19, 5687-5693.

(36) Peng, X.; Palma, S.; Fisher, N. S.; Wong, S. S. *Aquatic Toxicology* **2011**, 102, 186-196.

(37) Hu, Z.; Oskam, G.; Searson, P. C. *Journal of Colloid and Interface Science* **2003**, 263, 454-460.

(38) Brayner, R.; Ferrari-Iliou, R.; Brivois, N.; Djediat, S.; Benedetti, M. F.; FiÃ©vet, F. *Nano Letters* **2006**, 6, 866-870.

(39) Guo, L.; Ji, Y. L.; Xu, H.; Simon, P.; Wu, Z. *Journal of the American Chemical Society* **2002**, 124, 14864-14865.

(40) Yong-Jin Han, T.; Worsley, M. A.; Baumann, T. F.; Satcher, J. J. H. *Journal of Materials Chemistry*, 21, 330-333.

(41) Yang, K.; She, G.-W.; Wang, H.; Ou, X.-M.; Zhang, X.-H.; Lee, C.-S.; Lee, S.-T. *The Journal of Physical Chemistry C* **2009**, 113, 20169-20172.

(42) Adams, L. K.; Lyon, D. Y.; Alvarez, P. J. J. *Water Research* **2006**, 40, 3527-3532.

(43) Lin, D.; Xing, B. *Environmental Science & Technology* **2008,** 42, 5580-5585.

(44) Heinlaan, M.; Ivask, A.; Blinova, I.; Dubourguier, H.-C.; Kahru, A. *Chemosphere* **2008**, 71, 1308-1316.

(45) Xia, T.; Kovochich, M.; Liong, M.; MaÌˆdler, L.; Gilbert, B.; Shi, H.; Yeh, J. I.; Zink, J. I.; Nel, A. E. *ACS Nano* **2008**, 2, 2121-2134.

(46) Raghupathi, K. R.; Koodali, R. T.; Manna, A. C. *Langmuir* **2011**, 27, 4020-4028.

(47) Lindegren, M.; Loring, J. S.; Persson, P. *Langmuir* **2009**, 25, 10639-10647.

(48) Kilin, D. S.; Prezhdo, O. V.; Xia, Y. *Chemical Physics Letters* **2008**, 458, 113-116.

(49) Masui, T.; Hirai, H.; Imanaka, N.; Adachi, G.; Sakata, T.; Mori, H. *Journal of Materials Science Letters* **2002**, 21, 489-491.

(50) Goetze, T.; Gansau, C.; Buske, N.; Roeder, M.; Görnert, P.; Bahr, M. *Journal of Magnetism and Magnetic Materials* **2002**, 252, 399-402.

(51) Dakanali, M.; Raptopoulou, C. P.; Terzis, A.; Lakatos, A.; Banyai, I.; Kiss, T.; Salifoglou, *A. Inorganic Chemistry* **2002**, 42, 252-254.

(52) Wu, C.-M.; Baltrusaitis, J.; Gillan, E. G.; Grassian, V. H. *The Journal of Physical Chemistry C* **2011**, 115,10164-10172

(53) Rubasinghege, G.; Lentz, R. W.; Park, H.; Scherer, M. M.; Grassian, V. H. *Langmuir* **2009**, 26, 1524-1527.

(54) Max, J.-J.; Chapados, C. *The Journal of Physical Chemistry A* **2004**, 108, 3324-3337.

(55) Park, T.-J.; Levchenko, A. A.; Zhou, H.; Wong, S. S.; Navrotsky, A. *Journal of Materials Chemistry* **2010**, 20, 8639-8645.

(56) Liu, J.; Aruguete, D. M.; Jinschek, J. R.; Donald Rimstidt, J.; Hochella Jr, M. F. *Geochimica et Cosmochimica Acta* **2008**, 72, 5984-5996.

(57) Erbs, J. J.; Gilbert, B.; Penn, R. L. *The Journal of Physical Chemistry C* **2008**, 112, 12127-12133.

(58) Harbury, L. *Journal of Physical Chemistry* **1946**, 50, 190-199.

(59) Valtiner, M.; Borodin, S.; Grundmeier, G. *Langmuir* **2008**, 24, 5350-5358.

(60) Pasilis, S. P.; Pemberton, J. E. *Geochimica et Cosmochimica Acta* **2008**, 72, 277-287.

(61) García, A. B.; Cuesta, A.; Montes-Morán, M. A.; Martínez-Alonso, A.; Tascón, J. M. D. *Journal of Colloid and Interface Science* **1997**, 192, 363-367.

(62) In Zetasizer nano series technical note.

(63) Moayedi, H. A., A.; Moayedi, F.:Huat, B.K.B.; Kazemian,S. *International Journal of the Physical Sciences* **2011**, 6, 2004-2015.

(64) Guererro-Garcia, G. I. G.-T., E.; Chavez-paez, M.; Lozada-Cassou, M. *Journal of Chemical Physics* **2010**, 132, 54903.

(65) Domingos, R. F.; Tufenkji, N.; Wilkinson, K. J. *Environmental Science & Technology* **2009**, 43, 1282-1286.